Iowa Research Online
The University of Iowa's Institutional Repository

University of Iowa
Iowa Research Online

Theses and Dissertations

Spring 2014

Modeling and optimization of industrial systems with data mining

Xiaofei He
University of Iowa

Copyright 2014 Xiaofei HE

This thesis is available at Iowa Research Online: http://ir.uiowa.edu/etd/4645

Recommended Citation
He, Xiaofei. "Modeling and optimization of industrial systems with data mining." MS (Master of Science) thesis, University of Iowa, 2014.
http://ir.uiowa.edu/etd/4645.

Follow this and additional works at: http://ir.uiowa.edu/etd


Part of the Industrial Engineering Commons

MODELING AND OPTIMIZATION OF INDUSTRIAL SYSTEMS WITH DATA MINING

by

Xiaofei He

A thesis submitted in partial fulfillment
of the requirements for the Master of
Science degree in Industrial Engineering
in the Graduate College of
The University of Iowa

May 2014

Thesis Supervisor: Professor Andrew Kusiak

Copyright by

XIAOFEI HE

2014

All Rights Reserved

Graduate College
The University of Iowa
Iowa City, Iowa

CERTIFICATE OF APPROVAL

_____

MASTER'S THESIS

_____

This is to certify that the Master's thesis of

Xiaofei He

has been approved by the Examining Committee
for the thesis requirement for the Master of Science
degree in Industrial Engineering at the May 2014 graduation.

Thesis Committee: _____
Andrew Kusiak, Thesis Supervisor

_____
Yong Chen

_____
Pavlo A. Krokhmal

To My Parents

ACKNOWLEDGMENTS

First, I want to express sincere gratitude to my advisor, Prof. Andrew Kusiak. He has given me great support, invaluable advice and guidance in both research and studies. He instructed me with patience and taught me to how to conduct research. I appreciate experience at Intelligent System Laboratory, which prepared me for solving practical problems in industry.

I am grateful that Prof. Zijun Zhang for providing me an opportunity to work at City University of Hong Kong. He shared his successful research experience and provided invaluable suggestions for solving challenging problems.

I would like to acknowledge Prof. Yong Chen and Prof. Pavlo Krokhmal for serving my Thesis Committee and providing invaluable suggestions and feedback on my research.

I thank members of Intelligent System Laboratory who have worked with me. Special thanks to my colleagues: Yaohui Zeng, who worked with me on HVAC project and introduced me to this research area; Dr. Xiupeng Wei, who worked with me on wastewater project and shared his research experiences with me; Guanglin Xu, who discussed me with implementation of the HVAC optimization framework.

Finally and most importantly, I want to express thanks to my parents for their continuous, unconditional love and support.

ABSTRACT

Energy efficiency of industrial systems is of great concern to many. Modeling and optimization of industrial systems has been an active research area aiming at improvement of energy efficiency of these systems. Traditional analytical and physics-based methods, reported in literature, limit modeling industrial systems, which are complex, nonlinear, and dynamic.

Due to progress in data collection techniques, large volume of data has been collected and stored for analysis. Although much valuable information is contained in such data, utilization of the data in modeling industrial systems is lagging. Data mining is a novel science, providing a platform and techniques to model complex systems and processes. Data mining techniques have been widely applied in modeling various systems.

In this Thesis, two energy intensive industrial systems are investigated, a pump system in wastewater treatment plants, and an HVAC system in commercial buildings. Data mining is utilized to derive models describing the relationship between target, operational cost of systems, and system control variables. An optimization model is constructed to minimize operational cost of a system, and intelligent algorithms are employed to solve the optimization models. The study demonstrates a considerable energy saving by applying the proposed control strategy.

The approach developed in this Thesis can be applied to industrial systems other than the pump and HVAC systems.

TABLE OF CONTENTS

LIST OF TABLES

LIST OF FIGURES

CHAPTER 1

INTRODUCTION

Energy savings have become an important issue reducing costs and minimizing adverse impact on the environment. Numerous studies on energy savings in industrial facilities and processes have been reported in the literature [1–3]. In this thesis, industrial facilities of energy intensive are investigated, among those are pump system in wastewater treatment plants and heating, ventilation, and air conditioning (HVAC) system in commercial buildings.

It has been reported that approximately 3% of all electrical energy consumption in the United States and United Kingdom is typically accounted for electricity consumption by water and wastewater utilities [4]. Between 90% and 95% of the electricity purchased by water and wastewater utilities is used for pumping [5]. Consequently, optimizing management of pump system would lead to big economic benefits. The traditional operation of pump system is much dependent on experience of engineers, which leaves much space for energy savings using advanced management strategy. On the other hand, HVAC system is an important facility of buildings, providing heating, ventilation, and air conditioning to maintain comfort in buildings, as people spend large portion of time in buildings these days. The HVAC system consumes over 50% of the building energy in the US [6]. In most buildings, HVAC system is operated under full capacity all the time to meet peak load which happens occasionally. Energy savings are expected to operate HVAC system based on in-time load of buildings.

The development of data mining technology and data collection technique enable data-driven method to extract valuable information from historical data collected. The goal of this thesis is to achieve energy saving by optimizing management of pump system and HVAC system using data mining method.

1.1 Review of techniques for modeling and optimizing a pump system

The early research on pumps focused on the design of water distribution systems and pump control. The design research emphasized the minimization of costs. Alperovits and Shamir [7] optimized the design of a water distribution system using a linear programming gradient method. The proposed design aimed at minimizing the capital and operations cost of the water distribution system. Cunha and Sousa [8] investigated the design of a water distribution network with simulated annealing. Lansey and May [9] combined nonlinear programming and simulation in the design of a water distribution system. Studies on pump system control have focused on system efficiency. Ma and Wang [10] studied the control of variable speed pumps to optimize the energy efficiency of air-conditioning systems. Zhuan and Xia [11] applied model predictive control to a water pumping station. Ormsbee and Lansey [12] modeled and optimized the operations of a water supply system. The published studies on the design and operation of water distribution systems [7–12] have seldom considered energy savings.

The interest in energy savings for pumps is growing. Wang et al. [13] discussed scheduling the operations of water supply pumps using physics-based models. Zhuan and Xia [14] applied dynamic programming to schedule pumps with the objective of minimizing the total cost. Zhang et al. [15] studied ways to minimize the energy used by pumps in wastewater processing using data-driven models. Scheduling models have been solved using computational intelligence algorithms, including a genetic algorithm [16], particle swarm optimization [17], and ant colony optimization [18]. Van Zyl et al. [19] incorporated two hill-climbing strategies into a genetic algorithm to enhance the local search. Hajji et al. [20] integrated the scatter search, Tabu search, and neural network algorithms. A hybrid optimization algorithm was demonstrated at the Bouregreg water production system in Morocco. Lopez-lbanez et al. [21] introduced a variable coding scheme to reduce the search space compared to the binary representation in optimization.

To the author's knowledge, modeling characteristic of operating multiple pumps simultaneously is difficult and seldom investigated. The issue of scheduling pump system considering maintenance is also lack of attention.

1.2 Review of optimal control of a HVAC system

HVAC system has been an active area of the research, as it is one of the main energy consuming units in buildings. Typically, much efforts have been devoted to supervisory control these years, often named optimal control, which optimize HVAC system at the system level. Wang *et al* [22] gave a thorough review on supervisory control. Supervisory control can be classified to two categories, model-free supervisory control and model-based supervisory control. Model-based control can be further divided to physical based model control and black/gray-box model based supervisory control.

Model-free supervisory control develops no model, but control the system by rules generated by expert systems. Alcala et al. [23] proposed a fuzzy logic approach with rule weight derivation and rule selection to minimize the energy consumption of HVAC systems. Model-free supervisory control much depends on expert knowledge, which may suffer serious error out of knowledge of expert system. For model-based supervisory, based on physics, Lu et al. [24–25] formulated a global energy model by integrating energy models of the critical components of HVAC systems. Wang and Jin [26] studied the optimal control of an air-conditioning system using physics models. However, detailed physics models are complex and not suitable for online applications. Approaches other than physics-based models have been applied to optimize the performance of HVAC systems. Nassif and Moujaes [27] introduced a simple HVAC control strategy, selecting one of three pre-determined combinations of controller set points instead of solving physics-based models. Kusiak and Xu [28] applied a data-driven approach to construct a bi-objective optimization model for minimizing the energy consumption while preserving thermal comfort.

Although intensive discussions on minimizing the energy consumption of HVAC systems have been presented in the literature, the majority of research focused on optimization in a specified time interval, whereas optimization over long time horizons was rarely considered.

1.3 Applications of data mining methods in industry

Data mining is a powerful technique to discover and to reveal previously unknown, hidden, meaningful and useful patterns. [29]. Many engineering systems are not only energy intensive, and are becoming information intensive, as people realized the value of data.

Engineering systems generally have non-linear and complex characteristics. It is difficult to describe those systems using physical laws. However, data collected during the operation of systems contain those valuable information. Data mining technology has been applied in many industrial system management to improve efficiency of power usage, predict and diagnose system faults and so on. Koksal *et al.* [30] comprehensively reviewed the application of data mining techniques in manufacturing industrials. Fu X. and Cheng F. [31] applied data mining technique to improve building operational performance. Clustering analysis and association rules for extracting valuable information from data were studied and applicability was validated. Ilhami *et al* [32] utilized data mining method for wind turbine operation. Due to the stochastic nature of wind, the power generated by wind turbine is very difficult to predict, but data mining method gives good results in wind power predictions. In [33], Data mining method was applied for detection of system faults to avoid expense of inefficiency or failure of system. In [34], Data mining was used in predicting coefficient of performance (COP) for refrigeration equipment. Predicting coefficient of performance is useful in equipment monitoring, which lead to better performance of equipment.

Although data mining method has been widely applied to engineering field, it is still far from mature and advanced application in real systems. Further study is still required.

1.4 Thesis structure

The structure of the thesis is organized as follows. The first chapter introduced the background and goal of this thesis. Study on modeling and optimization of pump systems and HVAC systems has been reviewed in this section. And we reviewed application of data mining in industrial systems' operation. In chapter 2, pump system in a wastewater treatment plant was studied. Optimization model was constructed to help decide optimal pump system configuration and rotating speeds of pumps. Chapter 3 studied the scheduling of pump system considering maintenance of pumps. Maintenance decision of pump was modeled as a Markov decision process. In chapter 4, HVAC system in a commercial building is studied. Bi-objective optimization model considering both energy consumption and ramp rate of room temperature were presented. In the end, conclusion was made in chapter 5.

CHAPTER 2

OPTIMIZATION OF WASTEWATER PUMPING PROCESS WITH A DATA-DRIVEN APPROACH

2.1 Introduction

Pump system consumes considerable electricity in wastewater treatment plant. In this chapter, the pump system in a wastewater treatment plant is investigated. The objective is to compute and optimize the schedule of pump system in the preliminary process by minimizing energy consumption, while keeping the level of wet well chamber in a reasonable range.

Multiple layer perceptron (MLP) neural network is applied to model the pumping process of the pump system. The energy consumption models and outflow rate models of pump system configurations are derived from historical data. The optimization model is constructed by integrating those models and physical constraints, in which optimal pump system configuration and rotating speeds settings of pumps were decided. A pilot study optimizing pump system schedule presented by Zhang *et al* [15] achieved around 24.3% energy savings.

Due to the non-linearity and complexity of the optimization model, a computational intelligent algorithm, improved harmony search (IHS) [35] is utilized to solve the optimization model. Three scenarios are investigated, including low inflow rate scenario, medium inflow rate scenario, and high inflow rate scenario. Using the data collected from a wastewater treatment plant, considerable energy is saved in all three scenarios using the optimization model.

2.2 Pump configuration and data

The data used in this study is provided by Wastewater Reclamation Facility (WRF), located in Des Moines. In this plant, six pumps are used to lift waste water from the wet well chamber to preliminary process. Based on the inflow rate and level of wet well chamber, appropriate pump system configuration is selected, and proper pump speeds are set, which is controlled by the pre-programming PLC control.

The wastewater pumping process data used in this study is taken over the period from 1/1/2011 to 1/31/2013. The data is sampled with interval of 15 minutes. The data is processed to exclude errors and outliers. With six pumps, there are 26 = 64 pump system configurations in theory, including the configuration with all pumps are idle. In practical operation, five pumps at most can be simultaneously operated, and one or more pumps need to be used for backup. Further, the frequency of using different pump system configurations is not the same, resulting varied amount of historical data for different pump system configurations. To build statistical significant neural network models, sufficient data are necessary. With the data used in this study, 24 configurations with sufficient data are found. The data for each pump system configuration is summarized in Table 2.1. For configuration index C_{18}, for example, the description {5, 6} represents both pumps 5 and 6 are operated in configuration C_{18}.

Table 2.1. Pump configuration and corresponding data sets

Configuration Index	Description	Train	Test	Total	Configuration Index	Description	Train	Test	Total
C_1	{1}	6370	1592	7962	C_{13}	{2, 6}	290	73	363
C_2	{2}	4980	1245	6225	C_{14}	{3, 4}	280	70	350
C_3	{3}	5150	1287	6437	C_{15}	{3, 6}	503	126	629
C_4	{4}	6754	1688	8442	C_{16}	{4, 5}	4906	1227	6133
C_5	{5}	7644	1911	9555	C_{17}	{4, 6}	1926	482	2408
C_6	{6}	9136	2284	11420	C_{18}	{5, 6}	597	115	712
C_7	{1, 2}	430	108	538	C_{19}	{1, 3, 5}	194	49	243
C_8	{1, 4}	484	121	605	C_{20}	{1, 4, 5}	286	72	358
C_9	{1, 5}	289	72	361	C_{21}	{2, 4, 5}	254	64	318
C_{10}	{2, 3}	2003	503	2506	C_{22}	{2, 4, 6}	367	92	459
C_{11}	{2, 4}	706	176	882	C_{23}	{3, 4, 5}	377	94	471
C_{12}	{2, 5}	159	42	201	C_{24}	{1, 3, 4, 5}	266	66	332

2.3 Construction of a predictive model

To optimize the schedule of pump system, the relationship between output, energy consumption, and inputs, pump system configuration, rotating speeds of pumps, the level of wet well chamber, should be modeled. Different from physics based models, data-driven models are constructed. In expression (2.1) and (2.2), E_t represents the total energy of at a scheduling time window t, 15 min. $e_{i,t}$ represents the energy consumed using a single configuration C_i at time window t.

$$E_t = \sum_{i=C_1}^{C_{24}} e_{i,t} x_{i,t} \tag{2.1}$$

$$e_{i,t} = f_i(\mathbf{v}_{i,t}, l_{t-1}),\ i = C_1, ..., C_{24} \tag{2.2}$$

where i indicates the pump system configuration C_i shown in Table 2.1. $x_{i,t}$ is a binary parameter. $x_{i,t} = 1$ represents the pump system configuration C_i at time window t is selected for operating, and this configuration does not work if $x_{i,t} = 0$. Sum of $x_{i,t}$ should be 1 over i from C_1 to C_{24}, since only one configuration can be operated at a single time window. $\mathbf{v}_{i,t}$ is a vector of rotating speeds of pumps for configuration i at time t. l_{t-1} denotes the level of wet well chamber at time t-1. $f_i()$ represents the MLP neural network energy consumption model for configuration i.

Energy consumption model for each configuration is modelled using multiple layer perceptron (MLP) neural networks. The training dataset is used for training the model, while the test dataset is used for evaluating the accuracy of the model. As test result of configuration C_6 was shown in Figure 2.1, predicted energy consumption by MLP neural network is quite the same with the observed energy consumption, which indicats high accuracy of models built. Similar results can be found in Figure 2.2 for configuration C_{10}. Four metrics shown in Appendix A, MAE, sdAE, MAPE, and sdAPE, are used for evaluating the accuracy of predictive models. The testing result of all configuration were summarized in Table 2.2. From 2.2, MAPE of most models are less than 6%, which showed impressive accuracies of models.

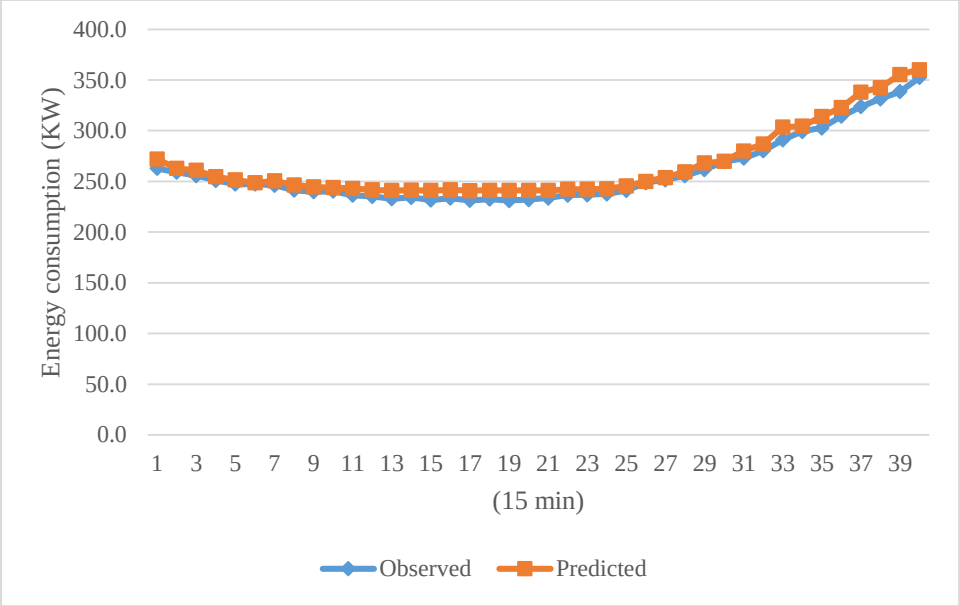

Figure 2.1. Observed and predicted energy consumption for C_6

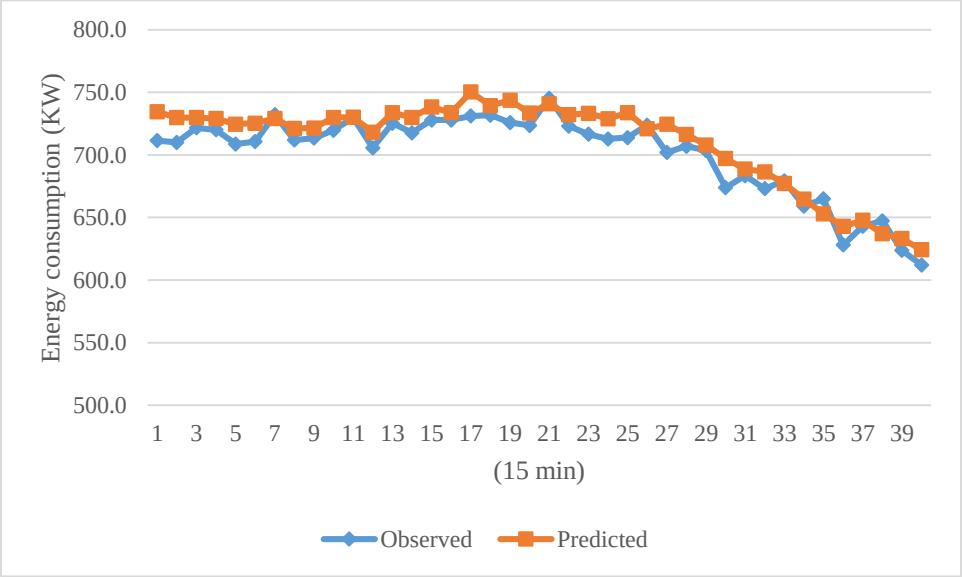

Figure 2.2. Observed and predicted energy consumption for C_{10}

Table 2.2. Accuracy of predictive models for energy consumption

Configuration Index	MAE	sdAE	MAPE	sdAPE	Configuration Index	MAE	sdAE	MAPE	sdAPE
C_1	7.77	7.16	2.33%	2.33%	C_{13}	13.77	10.99	2.43%	2.03%
C_2	38.66	12.43	11.39%	4.38%	C_{14}	6.84	5.14	1.27%	0.96%
C_3	18.73	14.95	5.11%	4.48%	C_{15}	13.46	21.8	2.33%	3.33%
C_4	12.24	10.77	3.72%	3.21%	C_{16}	3.78	3.89	0.72%	0.80%
C_5	21.67	16.92	6.04%	4.11%	C_{17}	17.18	12.32	3.03%	2.30%
C_6	11.63	8.66	3.29%	2.02%	C_{18}	17.2	12.62	3.52%	2.77%
C_7	20.02	15.43	3.19%	2.34%	C_{19}	9.24	7.01	1.06%	0.79%
C_8	5.49	5.05	0.85%	0.73%	C_{20}	8.93	6.41	0.79%	0.54%
C_9	9.64	10.04	1.19%	1.23%	C_{21}	7.83	6.63	0.72%	0.59%
C_{10}	10.74	7.46	1.72%	1.19%	C_{22}	12.82	10.62	1.35%	1.19%
C_{11}	11.91	8.71	2.17%	1.51%	C_{23}	9.00	6.56	0.95%	0.73%
C_{12}	11.95	7.1	2.32%	1.50%	C_{24}	8.28	6.16	0.53%	0.40%

Besides the energy consumption model, outflow rate models of pump configuration system are modelled using MLP neural networks. Outflow rate is modelled for monitoring the level of wet well chamber. The outflow rate model is shown in (2.3), and the level of wet well chamber is calculated in (2.4).

$$O_{i,t} = g_i(\mathbf{v}_{i,t}, l_{t-1}) \tag{2.3}$$

$$l_t = l_{t-1} + \frac{I_t - \sum_{i=C_1}^{C_{20}} O_{i,t} x_{i,t}}{A} \tag{2.4}$$

where $O_{i,t}$ represents the outflow rate by pump system configuration C_i at time window t; I_t denotes the inflow rate flowing into the wet well chamber at time window t; A represents the area of wet well chamber, and $g_i()$ is the MLP neural network model of outflow rate for configuration C_i.

The accuracy of outflow models are summarized in Table 2.3. Except for configurations C_2 and C_3, MAPE of models are smaller than 6%. The sdAPE of outflow rate model is a little bigger than that of corresponding energy consumption model, but the accuracies are still high. The plot showing the test accuracy of outflow rate model for configuration C_{18} is shown in Figure 2.2.

Table 2.3. Accuracy of outflow rate models

Configuration Index	MAE	sdAE	MAPE	sdAPE	Configuration Index	MAE	sdAE	MAPE	sdAPE
C_1	1.9	1.45	4.83%	4.42%	C_{13}	1.61	1.5	2.55%	2.45%
C_2	6.08	2.03	16.44%	9.32%	C_{14}	3.46	1.94	5.77%	3.42%
C_3	4.63	2.18	11.44%	7.63%	C_{15}	2.16	3.01	3.27%	4.32%
C_4	1.48	1.77	3.84%	5.64%	C_{16}	1.47	1.39	2.17%	2.15%
C_5	0.48	0.38	1.11%	0.89%	C_{17}	1.86	1.61	2.61%	2.18%
C_6	0.65	0.49	1.49%	1.20%	C_{18}	1.71	1.83	2.63%	2.52%
C_7	4.82	4.42	7.11%	6.86%	C_{19}	1.42	1.49	1.33%	1.39%
C_8	1.35	0.96	1.67%	1.10%	C_{20}	0.96	0.71	0.69%	0.51%
C_9	1.37	2.37	1.51%	3.87%	C_{21}	1.26	1.29	0.95%	0.96%
C_{10}	3.14	1.58	4.64%	2.45%	C_{22}	1.96	1.62	1.78%	1.51%
C_{11}	2.28	2.27	3.56%	2.74%	C_{23}	3.86	2.95	3.39%	2.77%
C_{12}	3.05	1.93	4.79%	3.09%	C_{24}	1.59	1.33	0.87%	0.74%

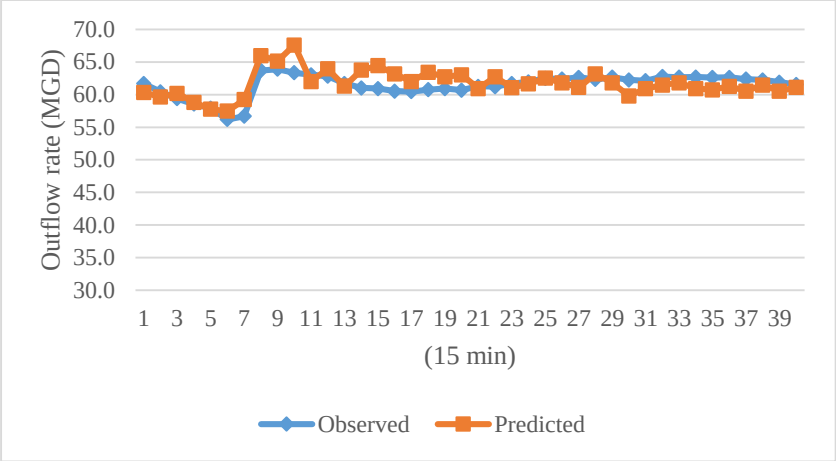

Figure 2.3. Observed and predicted outflow rate for configuration C_{18}

2.4 Optimization model

The energy consumption and outflow rate models trained by MLP neural networks are utilized to construct the optimization model of the pump system. The objective is to minimize the energy consumption by selecting the pump system configuration and controlling the rotating speeds of pumps. Meanwhile, some constraints have to be satisfied: 1) The level of wet well chamber should be restricted in a given range; 2) The change ratio of level of wet well chamber should be smaller than a given value, δ , to avoid big fluctuation of physical system; 3) Only one configuration can be operated at one time window; 4) The rotating speeds of pumps should be between 80% and 100% of full speed to keep efficiency of pumps; 5) In practical implementation, difference of rotating speeds between pumps under operating should be smaller than a given value, ε , for balancing load on pumps. Furthermore, predictive models would be more rigorous in this area with sufficient historical data. As illustrated in Figure 2.4, rather than optimized in a rectangle area formed by lowest and highest pump speed, the red filled area restricted by difference of speeds is optimized. In Figure 2.4, pump systems with 2 pumps are given, similar to pump systems with other multiple pumps.

Integrating equations (2.1) – (2.4) and constraints, the optimization model is constructed in model (2.5).

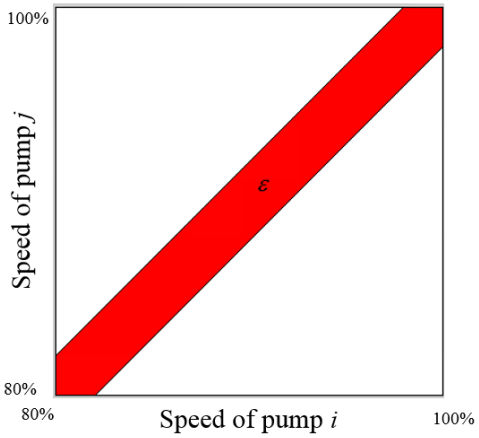

Figure 2.4. Optimization area of pump speeds for two pumps

$$
\begin{aligned}
&\min_{\mathbf{v}_{i,t},x_{i,t}} \; E_t \\
&\text{Subject to:} \\
&E_t = \sum_{i=C_1}^{C_{20}} e_{i,t} x_{i,t} \\
&e_{i,t} = f_i(\mathbf{v}_{i,t}, l_{t-1}) \\
&\sum_{i=C_1}^{C_{20}} x_{i,t} = 1 \\
&x_{i,t} = \{0,1\} \\
&O_{i,t} = g_i(\mathbf{v}_{i,t}, l_{t-1}) \\
&0.8 \le v_{ij,t} \le 1.0 \\
&\left| v_{ij,t} - v_{ik,t} \right| \le \varepsilon, \text{ for all } j \text{ and } k \text{ with } p_{ij,t} = 1 \text{ and } p_{ik,t} = 1 \\
&l_t = l_{t-1} + \frac{I_t - \sum_{i=C_1}^{C_{20}} O_{i,t} x_{i,t}}{A} \\
&l_{\min} < l_t < l_{\max} \\
&\left| l_t - l_{t-1} \right| < \delta
\end{aligned}
\tag{2.5}
$$

where $l_{\min}$ and $l_{\max}$ represent the lower and upper boundary of wet well chamber, respectively. $v_{ij,t}$

represents the speed of pump j in pump system configuration C_i, at time window t. $p_{ij,t} = 1$ indicates pump j in configuration i at time window t is running.

The model (2.5) consists of binary variables and continuous variables, besides nonlinear neural network models. Solving model (2.5) is challenging for conventional algorithms. Here, a computational algorithm, improved harmony search (IHS) [35] algorithm is applied to solve model (2.5).

Harmony search algorithm was first proposed by Z.W. Geem et al in 2001 [36], mimicking the process the improvisation of music players. Although it is a relatively new metaheuristic algorithm, its effectiveness and advantages have been demonstrated in various application. In this study, an improved harmony search algorithm is utilized to solve model (2.5), which employs a novel method for generating new solution vectors that enhances accuracy and convergence rate of harmony search (HS) algorithm. The steps in the procedures of IHS algorithm are presented as follows.

Step 1: Initialize parameters for IHS algorithm: HMCR, PAR, bw.

Step 2: Initialize harmony memory (HM) by randomly generating solutions.

Step 3: Improvise a new harmony.

Step4: Update the harmony memory.

Step5: Check the stopping criterion. Terminate if stopping criterion is satisfied; otherwise repeat Steps 3 to 5.

Each harmony represents a solution, and each pitch denotes one decision variable. HMCR is harmony memory consideration rate, which decides if the new pitch is selected from harmony memory, or generated randomly for the new harmony (solution). The PAR is pitch adjust rate,

which controls whether adjust will be applied to new generated pitch, while bw (band width) controls scale that the pitch is adjusted.

2.5 Computational results and discussion

From the data set described in Section 2.2, 360 instances are used for validating the capacity of saving energy of model (2.5). The inflow rate into the wastewater treatment plant would influence the pump operation and energy consumption. In this study, three scenarios are investigated considering level of inflow rate, low, medium and high, which were denoted with scenario 1, 2, and 3, respectively. The inflow rate for scenario 1 is ranging from 30 to 60 MGD. The inflow rate between 60 to 90 MGD is classified as scenario 2. And inflow rate of scenario 3 is from 90 MGD to 200 MGD.

Figures 2.5 and 2.6 show energy consumption and outflow rate by optimization in scenario 1. It is obvious that optimized energy consumption is consistently smaller than that consumed before optimization, as shown in Figure 2.5. In Figure 2.6, outflow rate by optimization is almost the same as observed value. This came from the fact the area of wet well chamber is small. To keep the level of wet well chamber, outflow rate has to be very close to the volume of inflow rate. The optimization result of the first 20 cases for pump system configuration and rotating speed of pumps for scenario 1 has been summarized in Table 2.5 in Appendix, in which first 20 cases are shown. From the table, pump system configuration is changed from pump 3 to pump 5. Since same amount of water are pumped, energy consumption in optimization is much less, which may be the reason that pump 5 was more energy efficient than pump 3.

The energy consumption savings can be observed in Figures 2.7 and 2.8 for scenarios 2 and 3. The first 20 cases of observed and optimized schedule for Medium and High inflow rate scenarios are summarized in Tables 2.6 and 2.7, respectively. The results demonstrated difference of energy efficiency between pump system configurations.

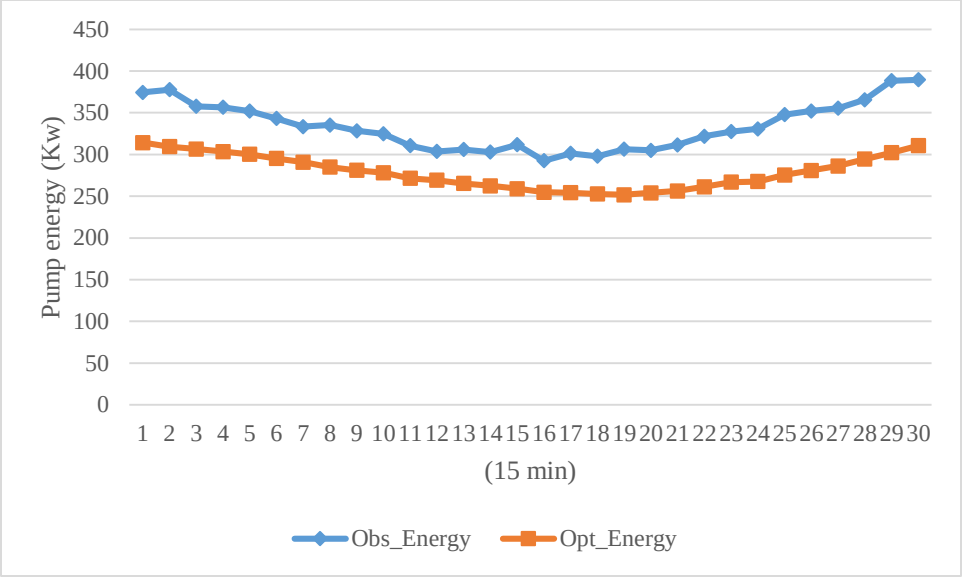

Figure 2.5.Observed and optimized energy consumption for scenario 1

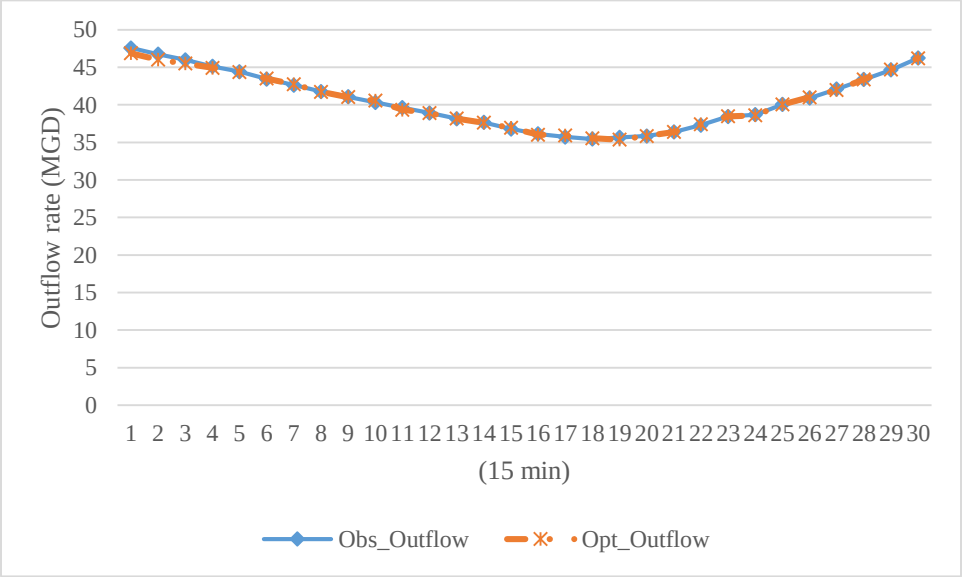

Figure 2.6. Observed and optimized outflow rate for scenario 1

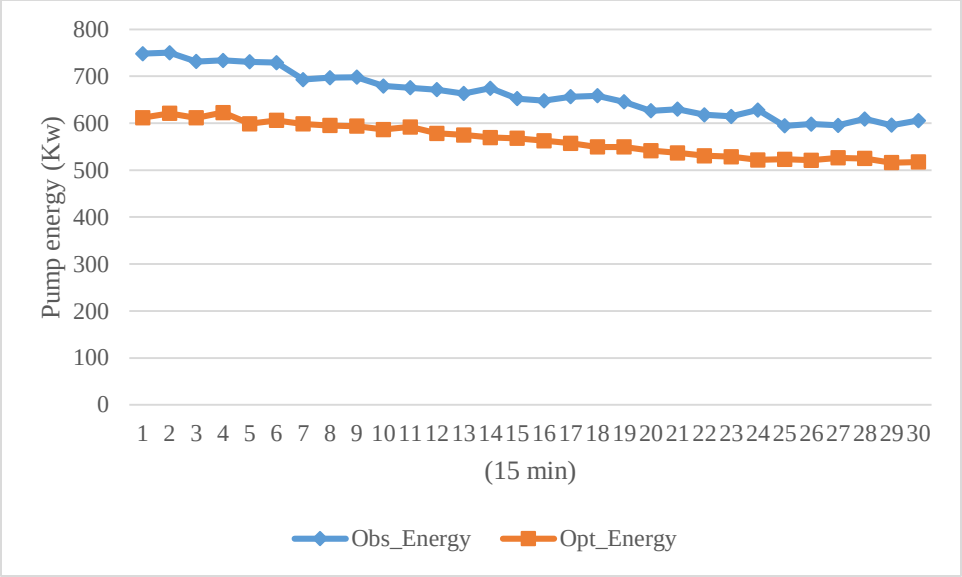

Figure 2.7.Observed and optimized pump energy consumption for scenario 2

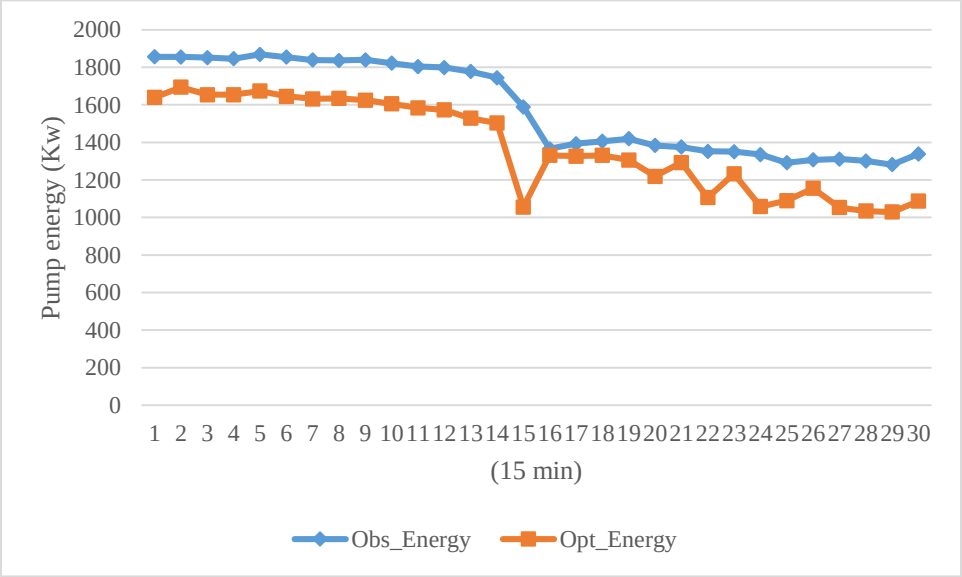

Figure 2.8. Observed and optimized pump energy consumption for scenario 3

120 cases with 15 minutes for each case are studied for each scenario. Therefore, 30 hours are studied for each scenario. The energy savings are presented in Table 2.3. Similar percentages of energy savings are obtained in three scenarios. More absolute energy savings are achieved in higher inflow rate scenario. The result validated the capacity of saving energy of the optimization model.

Table 2.4. Summary of energy saving by optimization

Scenario	Observed Energy (KWH)	Optimized Energy (KWH)	Energy Saved (KWH)	Energy Saved (%)
Scenario 1	11547.9	9411.7	2136.2	18.50%
Scenario 2	20249.5	17102.3	3147.2	15.50%
Scenario 3	35759.8	29892.3	5867.4	16.40%

Table 2.5. Observed and optimized pump schedule for scenario 1

Observed Pump Schedule						Optimized Pump Schedule					
Pump 1	Pump 2	Pump 3	Pump 4	Pump 5	Pump 6	Pump 1	Pump 2	Pump 3	Pump 4	Pump 5	Pump 6
-	-	92.12	-	-	-	-	-	-	-	89.59	-
-	-	91.57	-	-	-	-	-	-	-	89.12	-
-	-	91.07	-	-	-	-	-	-	-	88.84	-
-	-	91	-	-	-	-	-	-	-	88.53	-
-	-	89.05	-	-	-	-	-	-	-	88.23	-
-	-	89.7	-	-	-	-	-	-	-	87.76	-
-	-	89.2	-	-	-	-	-	-	-	87.34	-
-	-	88.53	-	-	-	-	-	-	-	86.8	-
-	-	88.37	-	-	-	-	-	-	-	86.44	-
-	-	87.86	-	-	-	-	-	-	-	86.18	-
-	-	87.47	-	-	-	-	-	-	-	85.55	-

Table 2.5. Continued

Observed Pump Schedule						Optimized Pump Schedule					
Pump 1	Pump 2	Pump 3	Pump 4	Pump 5	Pump 6	Pump 1	Pump 2	Pump 3	Pump 4	Pump 5	Pump 6
-	-	87.14	-	-	-	-	-	-	-	85.31	-
-	-	86.81	-	-	-	-	-	-	-	84.95	-
-	-	86.81	-	-	-	-	-	-	-	84.66	-
-	-	86.65	-	-	-	-	-	-	-	84.33	-
-	-	86.16	-	-	-	-	-	-	-	83.89	-
-	-	86.14	-	-	-	-	-	-	-	83.84	-
-	-	86.15	-	-	-	-	-	-	-	83.68	-
-	-	86.65	-	-	-	-	-	-	-	83.6	-
-	-	86.82	-	-	-	-	-	-	-	83.81	-

Table 2.6. Observed and optimized pump schedule for scenario 2

Observed Pump Schedule						Optimized Pump Schedule					
Pump 1	Pump 2	Pump 3	Pump 4	Pump 5	Pump 6	Pump 1	Pump 2	Pump 3	Pump 4	Pump 5	Pump 6
-	89.82	91.89	-	-	-	-	-	-	-	84.66	87.66
-	90.16	92.44	-	-	-	-	-	-	-	85.52	87.86
-	89.3	91.37	-	-	-	-	-	-	-	84.64	87.64
-	89.64	91.89	-	-	-	90.43	-	-	-	87.43	-
-	89.12	91.22	-	-	-	-	-	-	-	84.25	87.25
-	89.12	91.37	-	-	-	89.74	-	-	-	86.74	-
-	88.95	90.87	-	-	-	-	-	-	-	84.24	87.24
-	88.27	90.19	-	-	-	-	-	-	-	84.14	87.14
-	88.32	90.53	-	-	-	88.99	-	-	-	85.99	-
-	87.92	90.02	-	-	-	-	-	-	-	83.88	86.88
-	87.4	89.68	-	-	-	-	-	-	87.45	86.66	-
-	87.75	89.86	-	-	-	-	-	-	86.6	86.45	-
-	87.4	89.51	-	-	-	-	-	-	85.81	87.38	-
-	87.23	89.35	-	-	-	-	-	-	85.79	86.79	-
-	86.7	88.86	-	-	-	-	-	-	86.01	86.21	-
-	86.35	88.52	-	-	-	-	-	-	85.32	86.79	-
-	86.36	88.52	-	-	-	-	-	-	84.82	87	-

Table 2.6. Continued

Observed Pump Schedule						Optimized Pump Schedule					
Pump 1	Pump 2	Pump 3	Pump 4	Pump 5	Pump 6	Pump 1	Pump 2	Pump 3	Pump 4	Pump 5	Pump 6
-	86.25	88.51	-	-	-	-	-	-	84.48	86.61	-
-	86.19	88.52	-	-	-	-	-	-	84.59	86.47	-
-	85.85	87.81	-	-	-	-	-	-	85.01	84.8	-

Table 2.7. Observed and optimized pump schedule for scenario 3

Observed Pump Schedule						Optimized Pump Schedule					
Pump 1	Pump 2	Pump 3	Pump 4	Pump 5	Pump 6	Pump 1	Pump 2	Pump 3	Pump 4	Pump 5	Pump 6
100	97.36	99.88	88.35	-	-	93.41	-	96.41	95.55	95.25	-
100	97.7	99.88	88	-	-	96.46	-	93.52	95.38	93.46	-
100	97.53	99.88	88.17	-	-	94.58	-	91.89	96.69	96.66	-
100	97.52	99.88	88.16	-	-	94.62	-	96.3	94.88	95.21	-
100	97.59	99.88	88.17	-	-	96.56	-	98.37	93.56	93.56	-
100	97.71	99.88	88.17	-	-	97.31	-	94.31	94.31	94.31	-
100	97.71	99.89	88.17	-	-	95.96	-	93.46	94.86	94.72	-
100	97.71	99.88	87.32	-	-	97.09	-	94.09	94.09	94.09	-
100	97.53	99.89	87.15	-	-	96.75	-	93.75	94.13	93.75	-
100	97.7	99.88	85.96	-	-	96.49	-	93.49	93.49	93.49	-
100	97.54	99.89	85.62	-	-	93.92	-	94.67	93.89	92.77	-
100	97.72	99.89	85.78	-	-	95.82	-	92.82	92.82	92.82	-
100	97.71	99.89	84.94	-	-	91.03	-	92.2	93.83	92.59	-
100	97.71	99.89	83.59	-	-	91.23	-	89.49	92.8	94.23	-
-	97.72	99.89	94.36	-	-	-	-	89.6	89.98	91.5	-
-	92.79	95.3	95.72	-	-	86.67	-	89.45	89.67	89.67	-
91.41	86.95	89.34	90.08	-	-	86.54	-	89.54	89.54	89.54	-
91.73	87.28	89.67	90.58	-	-	86.58	-	89.58	89.58	88.81	-
91.92	87.46	89.67	90.59	-	-	86.84	-	89.84	87.96	88.9	-
91.21	86.75	89	89.9	-	-	95.57	-	-	92.57	98.57	-

CHAPTER 3

OPTIMIZATION OF OPERATIONS AND MAINTENANCE COST OF PUMPS

3.1 Introduction

In this chapter, a model for scheduling the operations and maintenance of pumps in wastewater processing is investigated. The energy consumption and maintenance cost are considered. The pump performance is modeled using data-mining algorithms rather than physical laws. The modeling capability of these data-mining algorithms has been demonstrated in numerous studies [37, 38]. The maintenance decision-making is formulated as a Markov decision process (MDP) [39]. The feasibility of using a Markov decision process in studying machine maintenance scheduling was presented in [40, 41]. The scheduling model includes a data-driven pump performance model and the MDP maintenance decision-making model. Because of the model complexity, an extended particle swarm optimization algorithm is applied to solve it.

3.2 Pump performance model

A pump system composed of six heterogeneous pumps used in a wastewater treatment process is investigated in this research. This pump system is responsible for delivering wastewater from a raw wastewater junction chamber to the primary treatment process. The six pumps are used in various operational configurations. Because of the pump heterogeneity and head influence [13, 42], it is challenging to develop a generic model for all of these operational configurations. Considering individual configurations may lead to more accurate models [15, 43]. In [15, 44], data-driven approaches were applied to model pump configurations. The energy consumption and wastewater outflow were modeled independently [15], which led to numerous models. In this paper, a new data-driven modeling strategy is introduced and tested.

3.2.1 Data description

To model the performance of pumps, a dataset collected from Jan 1, 2011 to Jan 31, 2013 is utilized. The data sampling interval is 15 min. The parameters in the dataset include the speeds of the six pumps, the junction chamber level, the wastewater outflow rate, and the energy consumption. The six pumps are indexed 1 to 6. The theoretical number of configurations for these six pumps is 62 [15]; however, only configurations with more than 190 data points are considered for modeling. Other configurations are discarded because of the insufficient data size. The dataset is then divided into subsets according to the pump configurations. Table 3.1 lists the pump configurations to be modeled and the corresponding datasets.

Table 3.1. Pump configurations and corresponding data sets

Configuration Index	Description	Training	Test	Configuration Index	Description	Training	Test
C_1	{1}	3638	862	C_{13}	{2, 6}	279	84
C_2	{2}	3636	864	C_{14}	{3, 4}	268	82
C_3	{3}	3640	860	C_{15}	{3, 6}	499	130
C_4	{4}	3598	902	C_{16}	{4, 5}	3605	895
C_5	{5}	3609	891	C_{17}	{4, 6}	1947	461
C_6	{6}	3623	877	C_{18}	{5, 6}	566	146
C_7	{1, 2}	438	100	C_{19}	{1, 3, 5}	199	44
C_8	{1, 4}	483	122	C_{20}	{1, 4, 5}	284	74
C_9	{1, 5}	293	68	C_{21}	{2, 4, 5}	238	80
C_{10}	{2, 3}	1994	512	C_{22}	{2, 4, 6}	346	113
C_{11}	{2, 4}	711	171	C_{23}	{3, 4, 5}	380	91
C_{12}	{2, 5}	165	34	C_{24}	{1, 3, 4, 5}	267	63

3.2.2 Modeling strategy

In this research, a multi-input multi-output (MIMO) model is developed to predict the energy consumption and wastewater outflow rate. A neural network algorithm [45] is applied to build the model. Figure 3-1 describes the proposed modeling strategy.

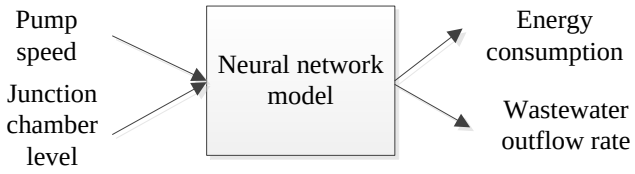

Figure 3.1. Proposed modeling strategy

The performance model of pump configuration *i* at time period *t* is formulated in (3-1).

$$y_{i,t} = f_i(\mathbf{x}_{i,t}, l_t), i = \mathrm{C}_1, \mathrm{C}_2, ..., \mathrm{C}_\mathrm{N}, t = 1, 2, ..., T \tag{3.1}$$

where $\boldsymbol{y}_{i,t} = (e_{i,t}, o_{i,t})^T$ and $\mathbf{x}_{i,t} = (x_{i,t}^1 s_t^1, x_{i,t}^2 s_t^2, ..., x_{i,t}^6 s_t^6)^T$, $x_{i,t}^j \in [x_{lb}, x_{ub}]$, $s_t^j \in \{0,1\}\ \forall i, j$. And e denotes energy consumption, o is wastewater outflow rate, function $f(\cdot)$ is MIMO model, input $\mathbf{x}$ is a vector of pump speeds, and l is the level of junction chamber. Variable s denotes status of pump. Pump is on with $s = 1$, otherwise, pump is off. Subscript i represents pump configuration i, and subscript t is time window t. The superscript j represents jth pump.

A function, $u_i(\cdot)$, is introduced to determine the selection of pump configuration i in a operation using strategy $\boldsymbol{s}_t$. By using $I_{(g_{i,j}=1)}(g_{i,j})$ as an indicator that pump j is operating in pump configuration i and $I_{(g_{i,j}=0)}(g_{i,j})$ to indicate that pump j is not selected, the general form of $u_i(\cdot)$ is expressed in (3.2).

$$u_i(\mathbf{s}_t) = \prod_{j=1}^{6}[I_{(g_{i,j}=1)}(g_{i,j}) s_t^j + I_{(g_{i,j}=0)}(g_{i,j})(1 - s_t^j)] \tag{3.2}$$

Expression (3.2) is intuitively explained next. If $i = \mathrm{C}_1$, then only pump 1 is operated according

to Table 3.1. Thus, only $g_{C_1,1}$ equals 1, and the remaining variables are 0. Then, $u_{c_1}(\cdot)$ is reformulated as $s_t^1(1-s_t^2)(1-s_t^3)(1-s_t^4)(1-s_t^5)(1-s_t^6)$, which ensures that pump configuration 1 is selected, if and only if s_t^1 is 1, while the remaining variables s_t^j are 0 for $j \neq 1$.

Based on Equations (3.1) and (3.2), the energy consumption of the pump system at t is computed according to (3.3).

$$E_t = \sum_{i=C_1}^{C_N} u_i(\mathbf{s}_t)(\mathbf{v}_e \mathbf{y}_{i,t}) \tag{3.3}$$

where $\sum_{i=C_1}^{C_N} u_i(\mathbf{s}_t) = 1$, $\mathbf{v}_e = (1,0)$, $\mathbf{s}_t = (s_t^1, s_t^2, ..., s_t^6)^T$, $s_t^j \in \{0,1\}, \forall j$. Similarly, the wastewater outflow rate of the pump system at time window *t* is expressed in (3.4).

$$F_t = \sum_{i=C_1}^{C_N} u_i(\mathbf{s}_t)(\mathbf{v}_f \mathbf{y}_{i,t}) \tag{3.4}$$

where $\mathbf{v}_f = (0,1)$.

The mass balance equation in (3.5) is utilized to compute the junction chamber level at the next time window based on the computed F_t. In (3.5), Q represents inflow rate, and A is area of junction chamber, and δ_0 denotes pump operation window.

$$l_{t+1} = \frac{(Q_t - F_t)\delta_0}{A} + l_t \tag{3.5}$$

3.2.3 Model validation

The dataset of each pump configuration in Section 3.2.1 was split into training and test datasets with ratios of 4/5 and 1/5, respectively, using random sampling. The models were trained using the training dataset and tested with the test dataset. The prediction accuracy of the developed models with measured using the following four metrics: 1) the mean absolute error

(MAE), 2) the standard deviation of the absolute error (sdAE), 3) the mean absolute percentage error (MAPE), and 4) the standard deviation of the absolute percentage error (sdAPE). These metrics are shown in Appendix A.

The accuracy of the developed model for each pump configuration in predicting the energy consumption and wastewater outflow rate is presented in Table 3.2. A comparison of these results with the results reported in studies [15] shows that MAE and MAPE are slightly improved, while sdAE and sdAPE are significantly reduced. Figures 3.2 – 3.5 show the energy consumption and wastewater outflow rate prediction accuracies for two randomly selected pump configurations.

Table 3.2. Prediction results for energy consumption and wastewater outflow rate

Configuration	Energy Consumption				Wastewater Outflow Rate			
	MAE	sdAE	MAPE	sdAPE	MAE	sdAE	MAPE	sdAPE
C_1	6.33	5.09	0.02	0.01	1.18	1.04	0.03	0.03
C_2	6.51	5.47	0.02	0.01	0.87	0.81	0.02	0.02
C_3	6.29	5.14	0.02	0.01	0.81	1.02	0.02	0.02
C_4	6.36	6.06	0.02	0.02	1.04	0.93	0.02	0.03
C_5	4.45	5.26	0.01	0.01	1.52	0.85	0.03	0.02
C_6	7.93	7.62	0.02	0.02	1.04	0.83	0.02	0.02
C_7	14.34	13.27	0.02	0.02	2	2.48	0.03	0.04
C_8	5.19	6.09	0.01	0.01	1.33	1.1	0.02	0.01
C_9	11.75	31.26	0.02	0.04	1.67	3.92	0.02	0.05
C_{10}	7.42	5.52	0.01	0.01	1.83	1.8	0.03	0.03
C_{11}	6.98	6.31	0.01	0.01	1.18	1.09	0.02	0.02
C_{12}	8.94	13.28	0.02	0.02	1.35	2.53	0.02	0.03
C_{13}	14.69	11.61	0.03	0.02	1.38	1.05	0.02	0.02
C_{14}	6.6	4.55	0.01	0.01	1.63	1.52	0.02	0.02
C_{15}	20.49	82.4	0.03	0.12	1.79	2.15	0.03	0.03
C_{16}	6.34	5.76	0.01	0.01	1.64	1.93	0.02	0.02
C_{17}	14.8	10.8	0.03	0.02	1.17	0.97	0.02	0.01
C_{18}	15.03	10.94	0.03	0.02	1.22	1.06	0.02	0.01

Table 3.2 Continued

Configuration	Energy Consumption				Wastewater Outflow Rate			
	MAE	sdAE	MAPE	sdAPE	MAE	sdAE	MAPE	sdAPE
C_{19}	6.67	5.66	0.01	0.01	1.39	1.11	0.01	0.01
C_{20}	8.34	5.81	0.01	0.01	1.31	0.96	0.01	0.01
C_{21}	10.13	6.39	0.01	0.01	1.57	1.3	0.01	0.01
C_{22}	14.8	13.28	0.01	0.01	3.31	4.81	0.03	0.04
C_{23}	12.29	10.09	0.01	0.01	2.97	2.02	0.02	0.02
C_{24}	7.8	5.72	0	0	1.14	0.94	0.01	0.01

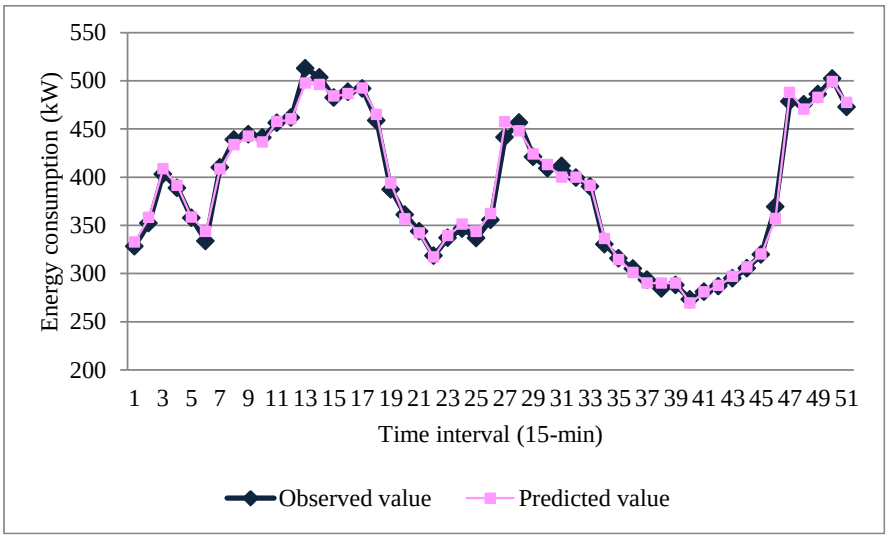

Figure 3.2. Observed and predicted energy consumption of configuration C_1

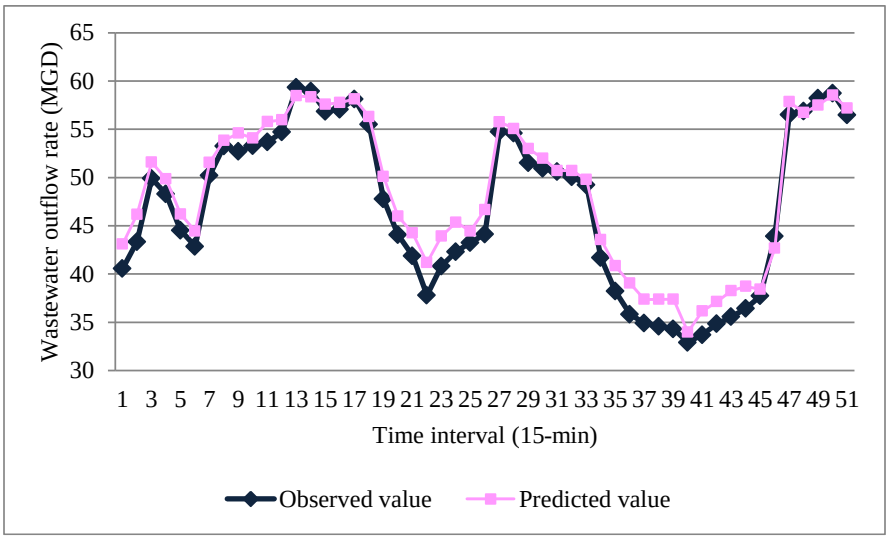

Figure 3.3. Observed and predicted wastewater outflow rates of C_1

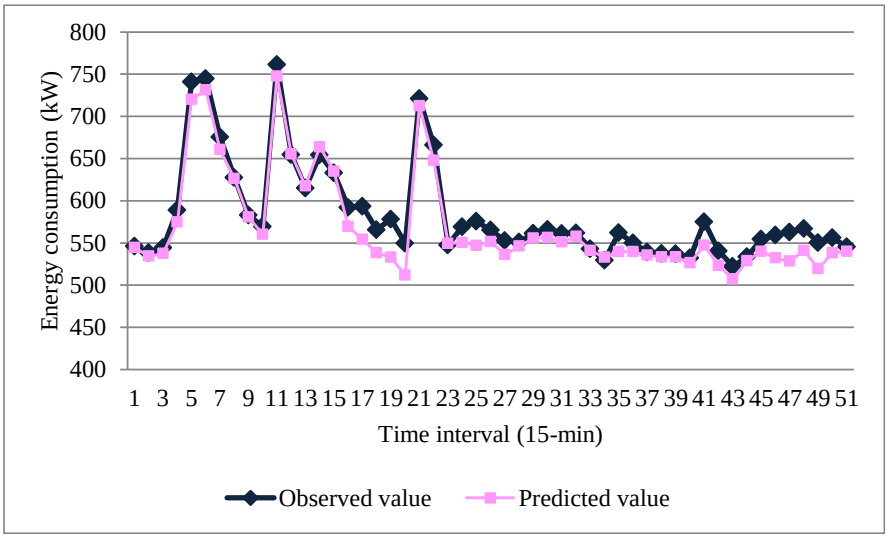

Figure 3.4. Observed and predicted energy consumption of C_7

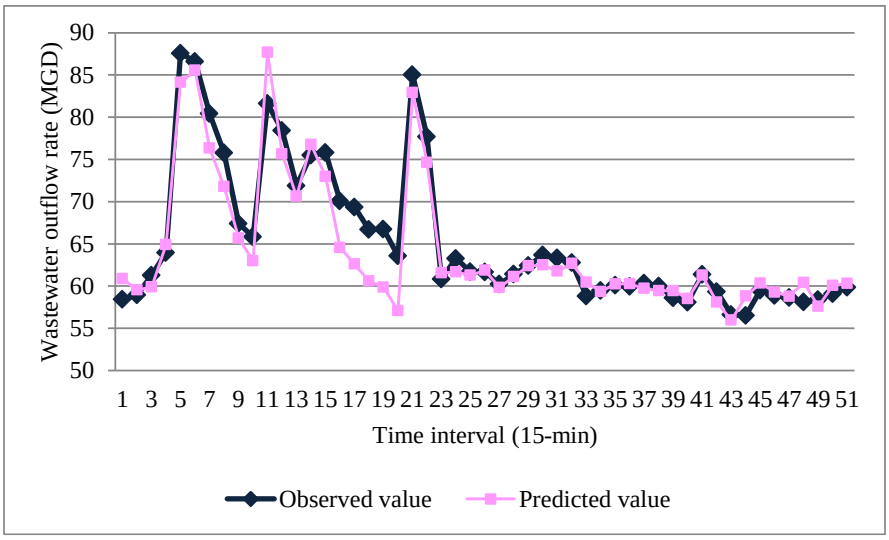

Figure 3.5. Observed and predicted energy consumption of C_7

3.3 Pump system maintenance model

A cost model for the maintenance of the pump system is introduced. A simplified maintenance scenario based on Assumptions 1 and 2 is considered.

Assumption 1.Maintenance is performed on only one pump in a single period.

Assumption 2. The maintenance time window, δ_m, is *n* times the operational time window, δ_0, $\delta_m = n\delta_0$, where $n > 1$.

In the pump system maintenance, decisions are made at two echelons. The first decision echelon, a decision vector, **d**, is introduced, and $\mathbf{d} = [d_1, d_2, d_3, d_4, d_5, d_6]$, $d_j \in \{0,1\}$, $j = 1,2,...,6$ and $\sum_{j=1}^{6} d_j = 1$, describes the selection of the j^{th} pump for maintenance. In the second echelon, two available maintenance actions need to be selected, a, $a \in \{1,2\}$. If $a = 1$, the pump will be repaired. If $a = 2$, the pump will be replaced by a new one.

3.3.1 Pump condition model

A Markov process is utilized to model the pump conditions with the maintenance action, a. Two states for the pump condition are considered: normal (state 1) and inefficient (state 2). Let $p^a_{n'm'}$ represent the probability of the pump condition transitioning from state n' to state m' under action a, $n', m' = 1, 2$, the corresponding transition matrix, $\mathbf{P}_a$, is expressed as (3.6).

$$\mathbf{P}_a = \begin{bmatrix} p^a_{11} & p^a_{12} \\ p^a_{21} & p^a_{22} \end{bmatrix}, a = 1, 2 \tag{3.6}$$

The operation of a pump impacts its condition. Thus, another matrix, $\mathbf{P}_o$, shown in Equation (3.7), is utilized to describe the transition probability of pump condition shifting.

$$\mathbf{P}_o = \begin{bmatrix} p^o_{11} & p^o_{12} \\ p^o_{21} & p^o_{22} \end{bmatrix} \tag{3.7}$$

3.3.2 Markov decision model

The cost of operating and maintaining pumps can be estimated based on the transition matrices, $\mathbf{P}_a$ and $\mathbf{P}_o$, using models (3.8) and (3.9). Because the maintenance data are unavailable, the transition matrices, $\mathbf{P}_a$ and $\mathbf{P}_o$, are assumed to be identical and independent for all pumps. A maintenance cost, R_a, is incurred by implementing action a. In addition, the states of the pump condition after maintenance leads to two state costs, r_1 $(r_1 = 0)$ and r_2. Based on the transition matrix, $\mathbf{P}_a$, and the costs, the expected cost of maintaining pump *j* with action a is formulated in Equation (3.8).

$$C(\mathbf{d}, a) = \sum_{j=1}^{6} d_j (R_a + p^a_{n'1} r_1 + p^a_{n'2} r_2),\ a = 1, 2,\ n' = 1, 2 \tag{3.8}$$

The $L(\mathbf{d}, s_t)$ in (3.9) is a pump operation loss function. Such a loss cost occurs when pumps

operate without maintenance.

$$L(\mathbf{d},\mathbf{s}_t)=\sum_{j=1}^{6} I_{(d_j=0)}(d_j) I_{(s_t^j=1)}(s_t^j)(p_{n'1}^{o} r_1 + p_{n'2}^{o} r_2) \tag{3.9}$$

In (3.9), $p_{n'1}^{o}$ and $p_{n'2}^{o}$ are the transition probabilities of operating pumps in states 1 and 2, respectively.

3.4 Maintenance and operations scheduling model

In this section, an optimization model is developed for scheduling the maintenance and operations of pumps.

3.4.1 Objective function

The maintenance and energy consumption costs are minimized in this study. A pump system performance model (3.3) is expressed in Section 3.2.2. However, because the first-echelon maintenance decision **d** impacts the availability of pump configurations, the total energy consumption of the pump system over the maintenance period is expressed in (3.10).

$$\mathbf{E(d,s}_t,\mathbf{x}_{i,t})=\sum_{t=1\delta_o}^{n\delta_o}\sum_{i=\mathrm{C}_1}^{\mathrm{C}_N}(1-\sum_{j=1}^{6} d_j s_t^j) u_i(\mathbf{s}_t)(\mathbf{v}_e\mathbf{y}_{i,t}),\ n\delta_o=\delta_m \tag{3.10}$$

According to (3.8)-(3.10), the total cost of maintaining and operating the pump system, V is estimated in (3.11).

$$V = C(\mathbf{d},a) + L(\mathbf{d},\mathbf{s}_t) + \mathbf{E(d,s}_t,\mathbf{x}_{i,t}) \tag{3.11}$$

3.4.2 Constraints

Several constraints are considered in scheduling. First, the ramp rate of the wastewater junction chamber level at *t* should not be lower than 0 or higher than a pre-determined threshold, l_θ, as expressed in (3.12).

$$0 < l_t < l_\theta \tag{3.12}$$

The absolute difference between the influent flow rate and the wastewater outflow rate should be less than a threshold, F_θ, as shown in (3.13). This constraint guarantees a smooth change in the junction chamber level, which is important in the wastewater delivery process.

$$\left|Q_t - F_t\right| \le F_\theta \tag{3.13}$$

The last important constraint is that for the pump speed settings discussed in Section 3.2.2.

3.4.3 Optimization model

Based on the objective function (3.11) and the constraints (3.12) and (3.13), the optimization model (3.14) is constructed.

$$\begin{aligned}
&\min_{\mathbf{d},a,\mathbf{s}_t,\mathbf{x}_{i,t}} V \\
&\text{s.t.} \\
&V = C(\mathbf{d},a) + L(\mathbf{d},\mathbf{s}_t) + \mathbf{E}(\mathbf{d},\mathbf{s}_t,\mathbf{x}_{i,t}) \\
&C(\mathbf{d},a) = \sum_{j=1}^{6} d_j (R_a + p^a_{n'1} r_1 + p^a_{n'2} r_2) \\
&L(\mathbf{d},\mathbf{s}_t) = \sum_{j=1}^{6} I_{(d_j=0)}(d_j) I_{(s_t^j=1)}(s_t^j)(p^o_{n'1} r_1 + p^o_{n'2} r_2) \\
&\mathbf{E}_{d_j} = \sum_{t=1\delta_o}^{n\delta_o} \sum_{i=\mathrm{C}_1}^{\mathrm{C}_N} (1 - \sum_{j=1}^{6} d_j s_t^j) u_i(\mathbf{s}_t)(\mathbf{v}_e \mathbf{y}_{i,t}) \\
&\mathbf{y}_{i,t} = f_i(\mathbf{x}_{i,t}, l_t) \\
&F_t = \sum_{i=\mathrm{C}_1}^{\mathrm{C}_N} u_i(\mathbf{s}_t)(\mathbf{v}_f \mathbf{y}_{i,t}) \\
&l_t = \frac{(Q_t - F_t)\delta_o}{A} + l_{t-\delta_o} \\
&\sum_{i=\mathrm{c}_1}^{\mathrm{c}_N} u_i(\mathbf{s}_t) = 1 \\
&\sum_{j=1}^{6} d_j = 1 \\
&\mathbf{x}_{i,t} = \left(x^1_{i,t} s^1_t, x^2_{i,t} s^2_t, ..., x^6_{i,t} s^6_t\right)^T \\
&x^j_{i,t} \in [x_{lb}, x_{ub}], s^j_t \in \{0,1\}, d_j \in \{0,1\}, \forall i, j \\
&0 < l_t < l_\theta \\
&|\, Q_t - F_t \,| \le F_\theta
\end{aligned} \tag{3.14}$$

The model (3.14) is transformed by applying a Lagrange multiplier, *M*, to constraints (3.12) and (3.13) [46].

In addition, because there are only six options in the first-echelon decision d_j, model (3.14) is reformulated as a master model (3.15) and six sub-models (3.16).

The master model can be formulated as follows:

$$\begin{aligned} &\min V \\ &\text{s.t.} \\ &V \in \{V_{d_1}, V_{d_2}, ..., V_{d_6}\} \end{aligned} \tag{3.15}$$

The six sub-models are represented as follows:

$$\begin{aligned} &\min_{a,\mathbf{s}_t,\mathbf{x}_{i,t}} V_{d_j} \\ &\text{s.t.} \\ &V_{d_j} = C(\mathbf{d},a) + L(\mathbf{d},\mathbf{s}_t) + \mathbf{E}_{d_j} + M\sum_{t=1\delta_o}^{n\delta_o}(\max\{0,0-l_t\} + \max\{0,l_t - l_\theta\} + \max\{0,|Q_t - F_t| - F_\theta\}) \\ &C(\mathbf{d},a) = \sum_{j=1}^{6} d_j(R_a + p^a_{n'1}r_1 + p^a_{n'2}r_2) \\ &L(d_j,\mathbf{s}_t) = \sum_{j=1}^{6} I_{(d_j=0)}(d_j) I_{(s_t^j=1)}(s_t^j)(p^o_{n'1}r_1 + p^o_{n'2}r_2) \\ &\mathbf{E}_{d_j} = \sum_{t=1\delta_o}^{n\delta_o}\sum_{i=C_1}^{C_N}(1-\sum_{j=1}^{6} d_j s_t^j)u_i(\mathbf{s}_t)(\mathbf{v}_e\mathbf{y}_{i,t}) \\ &\mathbf{y}_{i,t} = f_i(\mathbf{x}_{i,t}, l_t) \\ &F_t = \sum_{i=C_1}^{C_N} u_i(\mathbf{s}_t)(\mathbf{v}_f\mathbf{y}_{i,t}) \\ &l_t = \frac{(Q_t - F_t)\delta_o}{A} + l_{t-\delta} \\ &\sum_{i=c_1}^{c_N} u_i(\mathbf{s}_t) = 1 \\ &\mathbf{x}_{i,t} = \left(x^1_{i,t}s^1_t, x^2_{i,t}s^2_t, ..., x^6_{i,t}s^6_t\right)^T \\ &x^j_{i,t} \in [x_{lb}, x_{ub}], s^j_t \in \{0,1\}, \forall i \\ &d_j = 1 \\ &j = 1,2,3,...,6 \end{aligned} \tag{3.16}$$

After decomposition, only three types of variables, a, $\mathbf{s}_t$, and $\mathbf{x}_{i,t}$ are involved in model (3.16). the minimum of V can be obtained by solving model (3.16) iteratively with $d_j = 1$, from j = 1 to 6.

In (3.16), V_{d_j} is a linear combination of $C(\mathbf{d},a)$, $L(\mathbf{d},\mathbf{s}_t)$, $\mathbf{E(d,s}_t,\mathbf{x}_{i,t})$, and the penalty. Because $C(\mathbf{d},a)$ only involves variable *a*, and the left-over components only involve variables $\mathbf{s}_t$ and $\mathbf{x}_{i,t}$, the minimum of V_{d_j} can be decomposed as the minimum of $C(\mathbf{d},a)$ and the minimum of the left-over parts. The optimal maintenance action *a* is deterministic because of the value of $(R_1 + p^1_{n'1}r_1 + p^1_{n'2}r_2)/(R_2 + p^2_{n'1}r_1 + p^2_{n'2}r_2)$, a = 1, 2, n' = 1, 2. If the ratio is less than 1, the action a = 1 will be implemented. If the ratio is larger than 1, the action a = 2 will be implemented. If the ratio is equal to 0, either action can be implemented. Based on the minimum of $C(\mathbf{d},a)$, the optimal $\mathbf{s}_t$ and $\mathbf{x}_{i,t}$ need to be obtained to determine the minimum of V_{d_j}.

3.5 Extended particle swarm optimization algorithm

Solving model (3.16) is challenging for the following two reasons: 1) data-driven pump performance models are included, and 2) two types of variables, $\mathbf{s}_t$ (binary) and $\mathbf{x}_{i,t}$ (continuous), are involved. The mixed integer and highly nonlinear property significantly increase the complexity of model (3.16), and the traditional solution algorithms are not applicable. In this paper, a variable coding technique and extended particle swarm optimization algorithm are introduced to solve the proposed model (3.16).

3.5.1 Variable coding technique

In model (3.16), the number of binary and continuous variables increases with the number of operational time windows, *n*. A large value of *n* will lead to a high computational cost. Moreover, according to the dataset in Section 3.2.1, it can be observed that the number of feasible pump configurations for operation scheduling is limited. The iterative application of an algorithm to solve model (3.16) would lead to frequent infeasible combinations of binary variables.

A coding technique is utilized to reduce the number of binary variables and prevent infeasible solutions. An integer variable, $s_t^{'}$, is utilized to create a one-to-one map of the feasible values of the binary variable vector, $\mathbf{s}_t$, based on the available dataset in Section 3.2.1. For example, $s_t^{'} = 1$ means $\mathbf{s}_t = (1, 0, 0, 0, 0, 0)^T$. Therefore, if we let $s_t^{'}$ be the index of feasible pump configurations, searching for the optimal $\mathbf{s}_t$ is equivalent to searching for the optimal value of $s_t^{'}$. In estimating the value of the objective function, $s_t^{'}$ can be reversely translated into vector of binary values according to the one-to-one mapping.

3.5.2 Hierarchical particle swarm optimization

To search for the optimal values of $s_t^{'}$ and $\mathbf{x}_{i,t}$, a hierarchical particle swarm optimization (HPSO) is developed based on the modified discrete PSO [47] and canonical PSO [17]. This HPSO contains two PSO search layers. If we let $\mathbf{vs}^{'}$ and $\mathbf{vx}^{'}$ denote vectors of the candidate solution of $s_t^{'}$ and $\mathbf{x}_{i,t}$, the first and second search layers are presented as **Pseudo_Code_1_Layer** and **Pseudo_Code_2_Layer.**

Pseudo_Code_1_Layer:

```
run.PSO_1(N^p){
    vs′ = Initialization(N^p);
    count = 0;
    do{
        Fitness.cal(run.PSO_2(M^p,vs′),vs′, N^p);
        LocalBest(vs′, N^p);
        fit_1 = GlobalBest(vs′, N^p);
        Flight(vs′, N^p);
    }while(count ≤ G_c^1);
    Return(fit_1);
}
```

Pseudo_Code_2_Layer:

```
run.PSO_2(M^p, vs′){
    vx′ = Initialization(getDimension(vs′), M^p);
    count = 0;
    do{
        Fitness.cal(vx′, M^p);
        LocalBest(vx′, M^p);
        fit_2 =GlobalBest(vx′, M^p);
        Flight(vx′, M^p);
    }while(count ≤ G_c^2);
    Return(fit_2);
}
```

In the Pseudo_Code_1_Layer and Pseudo_Code_2_Layer, the function Fitness.cal() returns the value of the objective function of model (3.16) based on the partical vectors (candidate solutions), $\mathbf{vs}'$ and $\mathbf{vx}'$, initialized by Initialization() of size, N^p and M^p. LocalBest() and GlobalBest() update the local optimum of each particle and the global optimum of the swarm, respectively. Flight() iteratively varies the values of $\mathbf{vs}'$ and $\mathbf{vx}'$. If we let *k* be the index of particles, the procedure of Flight() in each iteration can be described as (3.17) and (3.18).

$$\upsilon_k = \omega\upsilon_k + h_1 q_1 (lbest_k - ps_k) + h_2 q_2 (gbest - ps_k) \tag{3.17}$$

$$ps_k = ps_k + \upsilon_k \tag{3.18}$$

In (3.17), ω = 0.5, h_1 = 2, and h_2 = 2 is applied according to [17]. The values of q_1 and q_2 are randomly generated from a uniform distribution, $U[0,1]$.

3.6 Case study

In the case study discussed in this section, the following maintenance scenarios are considered: a) the length of the maintenance time window is 3 h, the length of the operational time window is 15 min, and thus the value of *n* is 12; b) the initial pump condition state is 2; c)

the transition matrices, $\mathbf{P}_a$ and $\mathbf{P}_o$, a = 1, 2, are set as shown in (3.19); d) the values of R_1, R_2, r_1, and r_2 are set arbitrarily as the costs of consuming 200 kW, 600 kW, 0 kW, and 800 kW of electricity, respectively.

$$\mathbf{P}_o = \begin{bmatrix} 0.5 & 0.5 \\ 0 & 1 \end{bmatrix}, \mathbf{P}_1 = \begin{bmatrix} 1 & 0 \\ 0.8 & 0.2 \end{bmatrix}, \mathbf{P}_2 = \begin{bmatrix} 1 & 0 \\ 1 & 0 \end{bmatrix} \tag{3.19}$$

3.6.1 Algorithm convergence

One random instance from the dataset in Section 3.2.1 is considered to study the HPSO convergence. The termination criteria of the 1st and 2nd layer searches in HPSO are set to 1000 iterations. In the 2nd layer search, a pump configuration of three operating pumps is selected to check the convergence of the 2nd layer search. Figure 3.6 shows the result, and it can be observed that the 2nd layer search converges within 1000 iterations.

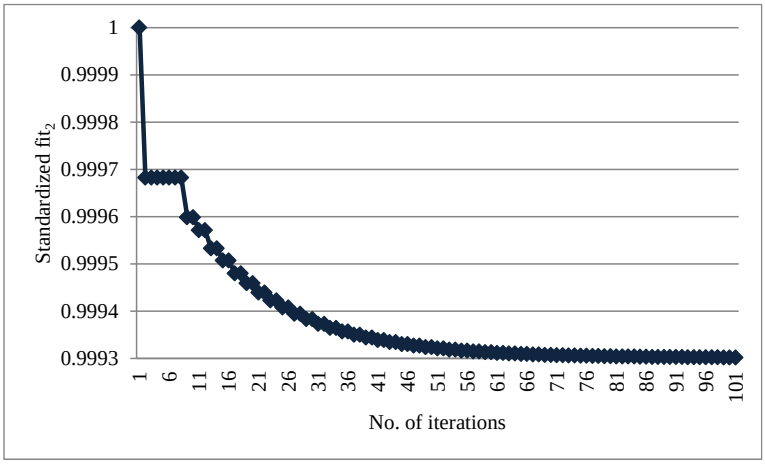

Figure 3.6. Convergence of 2nd layer search in HPSO

The convergence result of the 1st layer search in HPSO is shown in Figure 3.7. The 1st layer search can quickly converge (within 50 iterations) to local optimum based on the selected instance.

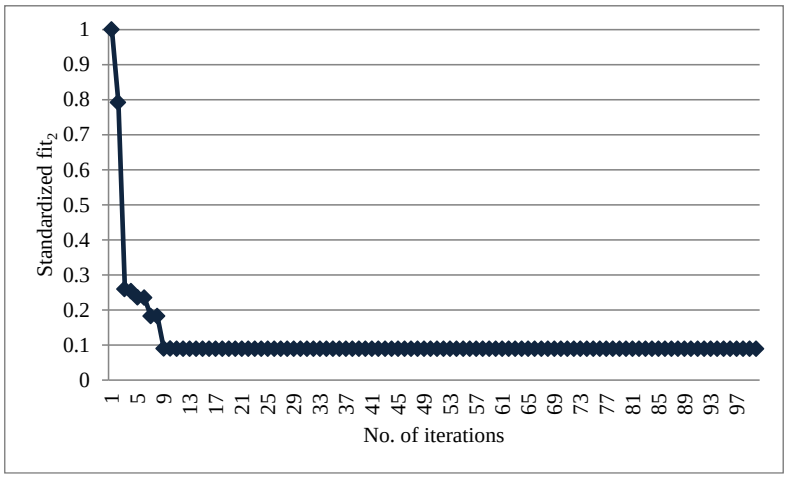

Figure 3.7. Convergence of 1st layer search in HPSO

The standardized fitness value in Figures 3.6 and 3.7 is calculated based on (3.20). The **fit** presents a vector of the best fitness obtained over the search.

$$\text{Standardized fitness} = \text{fit}/\max\{\mathbf{fit}\} \tag{3.20}$$

Based on the convergence results, in Section 3.6.3, the maximum numbers of iterations for implementing 1st layer and 2nd layer searches of HPSO are set to 100 and 50, respectively.

3.6.2 Computational instances

Three computational instances (CI1, CI2, and CI3) representing a low inflow-rate instance, medium inflow-rate instance, and high inflow-rate instance, are investigated. Each computational instance includes 12 operational time windows and 1 maintenance time window. The length of each operational time window is 15 min. Data from 12:30 am to 3:15 am on 1/10/2013 were selected for CI1 because the inflow rate was low, between 48 MGD and 60 MGD. Data from 13:30 pm to 16:15 pm on 2/14/2011 were selected for CI2. The inflow rate range during this period was 75–87 MGD. Data from 11:00 am to 13:45 pm were used for CI3 because of the high inflow rate, 150–160 MGD.

3.6.3 Computational results

The total cost of the pump system maintenance and operations with different d_j based on CI1−CI3 is summarized in Table 3.3. The optimal d_j that offers the lowest cost is shown in bold for the three computational instances. In CI1, pump 4 is recommended for maintenance because of having the lowest cost. Pump 3 is another option, even though its cost is slightly higher. In CI2, pump 6 is recommended for maintenance; however, maintaining pumps 2, 3, and 5 is also acceptable because of the low cost. In CI3, maintaining pump 1 involves the lowest cost. In some cases, Table 3.3 shows significant costs. This is because the maintenance of the corresponding pumps significantly affects the wastewater outflow rate and subsequently the junction chamber level. The maintenance action $a = 1$ is applied because it results in the lowest cost according to the fixed R_a and $\mathbf{P}_a$.

The pump operation schedules for the determined d_j for CI1−CI3 are presented in Table 3.4. The optimal pump configuration and optimal speed settings of the pumps in each operational time window are computed. When the wastewater inflow rate is low, operating one pump is preferred. When the wastewater inflow rate is higher, the operation of multiple pumps are required.

It is feasible to realize energy savings by scheduling operations and maintenance simultaneously. Table 3.5 presents the observed and computed energy consumption of the pump system. The positive and negative cost gains in Table 3.5 were estimated according to (3.21). An energy saving of approximately 9% was achieved in CI1, while a low energy savings or extra energy consumption was observed for CI2 and CI3. These results indicate that pump maintenance has a small impact on scheduling pump operations for low inflow rates; however, the impact becomes more significant when the wastewater inflow rate is high. It is also possible that the low energy savings are due to limited number of available pump configurations.

$$\text{Gain} = \frac{\text{Observed value} - \text{Computed value}}{\text{Observed value}} \times 100\% \tag{3.21}$$

A comparison of the computed and observed energy consumptions and computed junction chamber levels for CI1−CI3 is provided in Figures 3.8−3.13. It can be noted that a smoother junction chamber level could be achieved, as illustrated in Figures 3.9, 3.11, and 3.13, the computed junction chamber indicates a jump at the 9th time window. This is due to an increase in the junction chamber level without violating the constraints, leading to significant energy savings according to Figure 3.12.

Table 3.3. Pump maintenance decisions

CI1		CI2		CI3	
d_j	Cost (kW)	d_j	Cost (kW)	d_j	Cost (kW)
$d_1 = 1$	3263.36	$d_1 = 1$	3051.033	**$d_1 = 1$**	**2818.572**
$d_2 = 1$	2398.89	$d_2 = 1$	2618.574	$d_2 = 1$	3863.28
$d_3 = 1$	1993.68	$d_3 = 1$	2621.108	$d_3 = 1$	953870.8
$d_4 = 1$	**1992.71**	$d_4 = 1$	15592.65	$d_4 = 1$	5200.689
$d_5 = 1$	2810.64	$d_5 = 1$	2643.873	$d_5 = 1$	1931160
$d_6 = 1$	3447.86	**$d_6 = 1$**	**2613.138**	$d_6 = 1$	5072.16

Table 3.4. Computed schedules for three computational instances

Time Window	CI1		CI2		CI3	
	Pump Configuration	Speed Settings	Pump Configuration	Speed Settings	Pump Configuration	Speed Settings
1	{5}	{97.4}	{1,5}	{82.3, 96.6}	{2,4,5}	{93.5, 93.7, 90.2}
2	{1}	{97.8}	{1,2}	{88.8, 89.9}	{2,4,5}	{93.4, 93.7, 90.2}
3	{1}	{97.1}	{1,5}	{80.4, 97.3}	{2,4,5}	{93.5, 93.6, 89.3}
4	{1}	{96.7}	{2,4}	{81.2, 81.1}	{2,4,5}	{93.6, 93.5, 89.0}
5	{1,2}	{80.2, 98.9}	{2,5}	{80.8, 96.6}	{2,4,5}	{93.8, 93.5, 89.3}
6	{1,2}	{84.1, 94.7}	{2,4}	{80.0, 97.2}	{2,4,5}	{92.5, 94.0, 87.4}
7	{5}	{96.8}	{1,2}	{89.0, 97.6}	{2,4,5}	{93.9, 93.4, 89.4}
8	{1}	{91.7}	{1,5}	{86.3, 98.0}	{2,4,5}	{91.9, 94.8, 86.7}

Table 3.4. Continued

Time Window	CI1		CI2		CI3	
	Pump Configuration	Speed Settings	Pump Configuration	Speed Settings	Pump Configuration	Speed Settings
9	{1}	{93.6}	{2,5}	{81.6, 97.9}	{2,4,5}	{100.0, 83.4,83.6}
10	{1}	{93.6}	{1,5}	{86.6, 97.0}	{2,4,5}	{97.5, 89.1, 88.1}
11	{1}	{92.7}	{1,2}	{90.4, 94.5}	{2,4,5}	{92.7, 90.7, 82.7}
12	{5}	{91.3}	{1,5}	{87.2, 92.5}	{2,4,5}	{93.8, 90.4, 84.1}

Table 3.5. Pump energy consumption

Computational Instance	Computed Value	Observed Value	Gain
CI1 (kW)	432.71	474.76	8.86%
CI2 (kW)	646.57	581.47	-11.19%
CI3 (kW)	1218.01	1253.3	2.82%

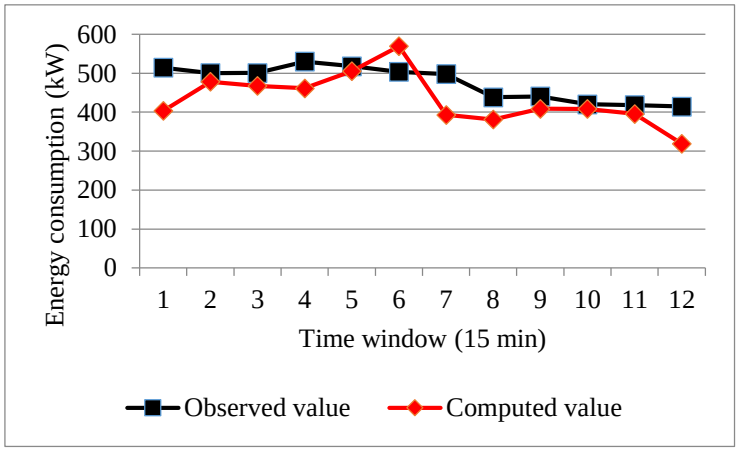

Figure 3.8. Computed and observe pump energy consumptions of CI1

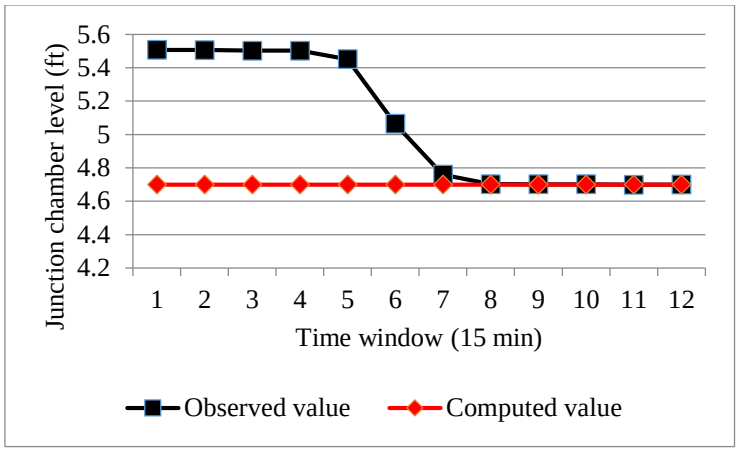

Figure 3.9. Computed and observed junction chamber levels of CI1

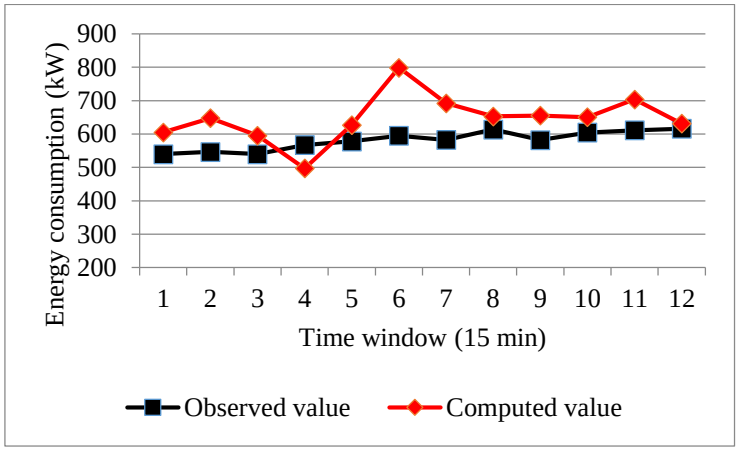

Figure 3.10. Computed and observe pump energy consumptions of CI2

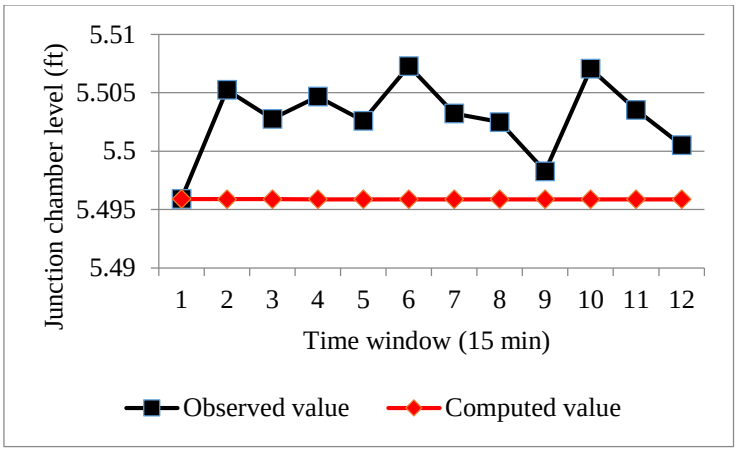

Figure 3.11. Computed and observed junction chamber levels of CI2

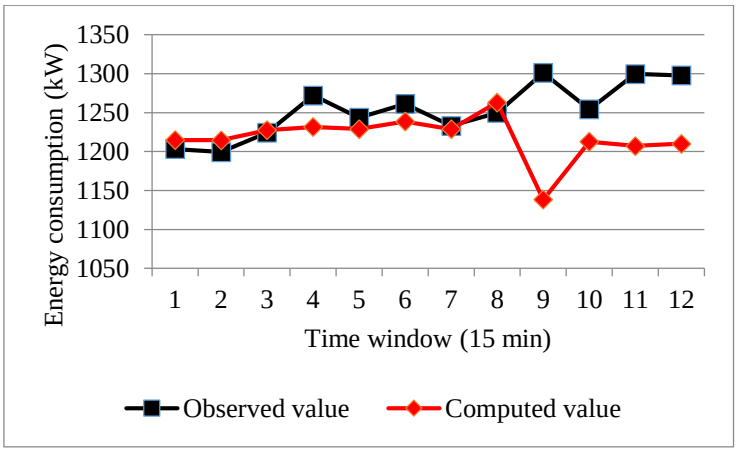

Figure 3.12. Computed and observe pump energy consumptions of CI3

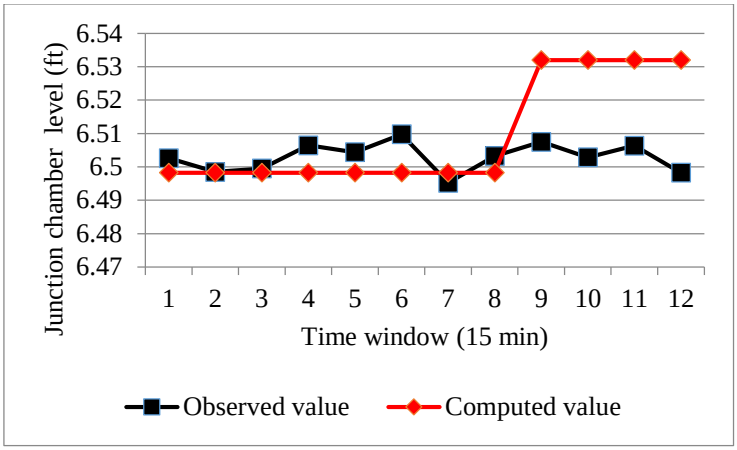

Figure 3.13. Computed and observed junction chamber levels of CI3

3.7 Conclusion

In this chapter, the maintenance and operations of pumps in a wastewater processing plant were studied. An optimization model was developed to optimize the maintenance and operational schedules. Asynchronous time windows for the maintenance and operations scheduling were considered. A Markov decision process was utilized to develop the maintenance decision-making model. A data-driven approach was utilized to model the pump system performance. The junction chamber level in the wastewater treatment was constrained in the optimization of the pump operation and maintenance scheduling.

In solving the scheduling model, a variable coding technique was applied to reduce the number of variables. Because of the model complexity, a hierarchical particle swarm optimization (HPSO) algorithm was developed. The proposed HPSO algorithm include two layers. The first layer aims at obtaining an optimal solution for the integer variables. The second PSO search layer obtains an optimal solution for the continuous variables. The computational results from solving the maintenance and operations scheduling model were provided. The optimal maintenance decision, maintenance action, and operational schedule were presented. The

results indicated that energy savings were possible. In addition, the variation in the junction chamber level was smoothed.

CHAPTER 4

PERFORMANCE OPTIMIZATION OF HVAC SYSTEM WITH COMPUTATIONAL INTELLIGENCE ALGORITHM

4.1 Introduction

Although intensive discussions on minimizing the energy consumption of HVAC systems have been presented in the literature, the majority of research focused on optimization in a specified time interval, whereas optimization over long time horizons was rarely considered. In this chapter, energy saving model in long time horizon was studied by considering objectives, both energy consumption and room temperature ramp rate (TRR).

A room temperature ramp rate (TRR) expresses the change of room temperature over a time interval, e.g., 15 min. The minimization of the energy consumption only at a given time interval may result in significant fluctuations of the room temperature, reduce the energy saving space, and even increase the future energy consumption. A well control of TRR is beneficial to smooth the settings of the HVAC controlled parameters and stabilize the energy saving in a long run. This study aims to investigate the HVAC system performance optimization by considering two objectives, the minimization of the total energy consumption and average TRR, through improving the control. The total energy consumption consists of energy consumed by air handling units (AHU), chillers, pumps, and fans. The average TRR is the mean TRR of five considered rooms. A data-driven approach is applied to build predictive models of energy consumption and average TRR. The accuracy of the predictive models is validated. In the control, two set points are optimized, the discharged air temperature set point (DAT-SP) and the supply air static pressure set point (SASP-SP), in order to discover the more suitable balance between air flow rate and inlet temperature in five rooms, reduce the total energy consumption, and ensure comfort. The variable air volume (VAV) boxes are controlled by the default proportional integral derivative (PID) controller.

A performance optimization model is introduced by incorporating the data-driven predictive models and constraints. Solving the proposed optimization model with traditional solution algorithms is challenging because of the complexity and nonlinearity. Thus, three computational intelligence (CI) algorithms are considered for the model solving: an evolutionary algorithm [48, 49], a particle swarm optimization [17], and a harmony search algorithm [35, 36]. The performance of these algorithms depends on their parameter settings. The design and analysis of computer experiments (DACE) [50, 51] is introduced to generate 300 samples of parameter settings for each algorithm to compare three CI algorithms. Five instances are considered in the evaluation. The best performing CI algorithm is selected to optimize the HVAC system's performance. Three cases are investigated in this study to demonstrate the improvement in the HVAC system's performance. The computational results are assessed by comparing with the baseline strategies. Significant energy savings are demonstrated. The benefit of TRR as a factor in energy optimization for a long-time horizon is validated.

4.2 Predictive models of HVAC systems

4.2.1 System description

This study was conducted in a commercial building, the University Service Building (USB) at the University of Iowa. In the USB, one air handling unit (AHU) is responsible for heating, air conditioning, and ventilation of the entire building which has a gross floor area of 71,123 ft² (6607 m^2). The AHU was operated by setting the default constant values, i.e., 55 °F (12.78 °C) and 2.3 in. WG (0.57 kPa), respectively, to the temperature set point (DAT-SP) and the static pressure set point (SPSA-SP). To monitor whether the building temperature was well controlled, five representative rooms (Rooms 1–5) sensitive to the thermal load were selected. Once the room temperatures of these five representative rooms were within predefined ranges, the thermal comfort of the building was considered under control.

The default values of two controlled setting points were determined for handling the peak load. However, based on such control setting, the HVAC system runs at its full capacity even at a

partial load. Therefore, by optimally adjusting the two controlled set points, energy savings are expected. To construct a performance optimization model, the relationships between the two controlled set points and the energy consumption, as well as the temperature of five rooms, need to be established.

4.2.2 Building predictive models

As two controlled set points were fixed at the USB, a data collection experiment was conducted to collect data of the HVAC system and the values of the two controlled set points were adjusted over time. The experiment was carried out during an occupancy period, from 8:00 a.m. to 6:00 p.m., Monday to Friday, from May 20 to July 1, 2013. The ranges of DAT-SP and SASP-SP were 55–60 °F (12.78–15.56 °C) and 1.8–2.3 in. WG (0.45–0.57 kPa), respectively. Because complaints about high room temperatures were reported on June 3, the range of DAT-SP was scaled down while the range of SASP-SP was maintained for the follow-up experiment period. The two controlled set points were modified every 15 min. At each modification, the values of the two controlled set points were randomly generated from their corresponding ranges. Next, the generated values were written into the controller of the AHU at the USB.

The values of the parameters of the air handling unit (AHU) were recorded with 1-min sampling intervals. The dataset collected in the experiment was then averaged to 15-min intervals for modeling. After data pre-processing, the dataset was split into randomly sampled training (80% of the data) and test (20% of the data) sets. Six predictive models, the energy consumption model of the HVAC system and five room temperature models, were built. The feasibility of using these models in a real application was further validated by using data collected from July 9 to July 11, 2013.

Table 4.1 summarized the parameters used in the predictive models. The parameters were categorized into three groups: controlled parameters, uncontrolled parameters, and target parameters. The target parameters were the outputs of the predictive models. The historical

values of the target parameters were also included as inputs to improve the prediction accuracy of the models. The six predictive models have the form shown in (4.1) and (4.2).

$$E_{t+d} = g(\mathbf{x}_{t+d}, E_t, \mathbf{x}_t, \mathbf{u}_t) \tag{4.1}$$

$$T_{t+d} = f_i(\mathbf{x}_{t+d}, T_{t,i}, \mathbf{x}_t, \mathbf{u}_t) \tag{4.2}$$

where E denotes computed energy consumption, T represents room temperature, $\mathbf{x}$ is an vector of control variables, and $\mathbf{u}$ is an vector of uncontrolled variables. Subscripts t denotes time, and d is a time interval (15 min), and subscript i is an index of representative room.

The multi-layer perceptron (MLP) neural network [52, 53] was selected to construct the predictive models because a previous study [27] demonstrated that it outperformed other data mining algorithms. The four metrics defined in Appendix I were used to evaluate the performance of the predictive models. the mean absolute error (MAE), the standard deviation of absolute error (sdAE), the mean absolute percentage error (MAPE), and the standard deviation of absolute percentage error (sdAPE).Table 4.2 lists the test results of the predictive models. The MAPE of the energy predictive model was 5.19%, which indicated an accuracy of nearly 95%. The prediction accuracy for the five models of room temperature was as high as 99%. These high accuracy models were then utilized to construct the optimization model discussed in Section 4.4. The validation results in Table 4.3 illustrated that all the models have high prediction accuracy. According to Tables 4.2 and 4.3, the MAPE and sdAPE of the testing and validation results are similar for all the models. Therefore, the developed data-driven models can be utilized in simulations to aim at providing insights into the operations of HVAC systems.

Table 4.1. Summary of parameters for predictive models

Parameter Type	Parameter Name	Description	Unit
Control parameters	SASP-SP	Static pressure set point	In.WG
	DAT – SP	Discharged air temperature set point	°F
Uncontrolled parameters	OA –Temp	Outside air temperature	°F
	S-CFM	Supply air flow	CFM
	CTG-TEMP	Air temperature after cooling coil	°F
	CLG-VALVE	Cooling valve control	%Open
	HTG-TEMP	Air temperature after heating coil	°F
	MA-TEMP	Mixed air temperature	°F
	RA-TEMP	Return air temperature	°F
	HWS-TEMP	Heating water supply temperature	°F
	HWR-TEMP	Heating water return temperature	°F
	CW-S-T	Cooling water supply temperature	°F
	CW-R-T	Cooling water return temperature	°F
Target parameters	E	Energy	KWH
	Rm1 ZN-T	Room 1 temperature	°F
	Rm2 ZN-T	Room 2 temperature	°F
	Rm3 ZN-T	Room 3 temperature	°F
	Rm4 ZN-T	Room 4 temperature	°F
	Rm5 ZN-T	Room 5 temperature	°F

Table 4.2. Test results of predictive models

Model	MAE	Sd_AE	MAPE	Sd_APE
Energy	1.74	2.05	5.19%	7.28%
Rm1 ZN-T	0.14	0.14	0.20%	0.20%
Rm2 ZN-T	0.14	0.38	0.20%	0.50%
Rm3 ZN-T	0.09	0.09	0.10%	0.10%
Rm4 ZN-T	0.15	0.23	0.20%	0.30%
Rm5 ZN-T	0.18	0.17	0.20%	0.20%

Table 4.3. Validation results of predictive models

Model	MAE	Sd_AE	MAPE	Sd_APE
Energy	2.18	1.65	4.59%	3.66%
Rm1 ZN-T	0.12	0.08	0.17%	0.11%
Rm2 ZN-T	0.11	0.07	0.15%	0.10%
Rm3 ZN-T	0.06	0.05	0.08%	0.07%
Rm4 ZN-T	0.14	0.12	0.18%	0.15%
Rm5 ZN-T	0	0	0.24%	0.20%

4.3 Formulation of optimization model

This study has focused on improving the performance of an HVAC system by achieving two objectives: the minimization of its energy consumption and the average ramp rate of the room temperature. To meet the system and thermal comfort requirements, the following conditions need to be satisfied:

(1) The value of DAT-SP can vary from 55 to 58 ℉ (12.76–14.44 °C);

(2) The value of SASP-SP can vary from 1.8 to 2.3 in. WG (0.45–0.57 kPa) ;

(3) The room temperature of each representative room should fall between the pre-determined lower bound and upper bound to ensure thermal comfort.

The constraints of the room temperatures and control parameters are expressed in (4.3) and (4.4).

$$\mathrm{L}_{T,\mathrm{i}} \le T_{t,i} \le U_{T,i} \tag{4.3}$$

$$\mathbf{x}_l \le \mathbf{x}_{t+d} \le \mathbf{x}_u \tag{4.4}$$

In studies [54, 55], a local optimization model was established by considering only one objective, minimizing the energy consumption over a time interval. However, optimization over a single time interval may not result in overall energy savings. This is due to the fact that optimization over one time interval may diminish the payoff over the subsequent time intervals. For example, the operator can set the lowest value of SASP-SP and the highest value for DAT-SP (when the HVAC system operates at its lowest capacity) over a current time interval to maximize the reduction of the energy consumption while maintaining the thermal comfort within a pre-determined threshold. Although significant energy savings could be achieved in the current

time interval, such a control strategy will increase the room temperature, and subsequently diminish the potential for energy savings or even increase the energy consumption at future time intervals. To achieve energy savings in HVAC systems in the long run, minimization of the room temperature ramp rate (TRR) in each time interval is considered as another objective. Moreover, the reduction of the room temperature ramp rate will prevent setting controllable parameters at their boundaries and smooth the control over time.

The two objectives, minimization of the energy consumption and the average TRR of five representative rooms, constitute the objective function. The energy consumption is normalized to [0, 1] according to (4.5). The minimum and maximum values of the observed energy consumption in the dataset are utilized.

$$O_1 = \frac{E_{t+d} - \min\{\mathbf{E}\}}{\max\{\mathbf{E}\} - \min\{\mathbf{E}\}} \tag{4.5}$$

where **E** is a vector of observed energy consumption.

The average TRR is computed by model (4.6) and normalized to [0,1] according to (4.7). The threshold, ξ, is the allowable maximum room temperature ramp rate. m is the total number of representative rooms.

$$R_{t+d,i} = \frac{\left|T_{t+d,i} - T_{t,i}\right|}{\xi} \tag{4.6}$$

$$O_2 = \frac{\sum_{i=1}^{m} R_{t+d,i}}{m} \tag{4.7}$$

By incorporating data-driven models ((4.1) and (4.2)) and constraints ((4.3) – (4.7)), the optimization model is formulated as (4.8). Coefficient, w, is utilized to distribute weights between two objectives, O_1 and O_2.

$$
\begin{aligned}
&\min wO_1 + (1-w)O_2 \\
&\text{s.t.} \\
&O_1 = \frac{E_{t+d} - \min\{\mathbf{E}\}}{\max\{\mathbf{E}\} - \min\{\mathbf{E}\}} \\
&O_2 = \frac{\sum_{i=1}^{m} R_{t+d,i}}{m} \\
&R_{t+d,i} = \frac{\left|T_{t+d,i} - T_{t,i}\right|}{\xi} \\
&E_{t+d} = g(\mathbf{x}_{t+d}, E_t, \mathbf{x}_t, \mathbf{u}_t) \\
&T_{t+d,i} = f_i(\mathbf{x}_{t+d}, T_{t,i}, \mathbf{x}_t, \mathbf{u}_t) \\
&L_{T,i} \le T_{t,i} \le U_{T,i} \\
&\mathbf{x}_l \le \mathbf{x}_{t+d} \le \mathbf{x}_u \\
&w \in [0,1]
\end{aligned}
\tag{4.8}
$$

4.4 Computational intelligence algorithms

As the optimization model in (4.8) includes MLP neural network models, it cannot easily solved with traditional optimization algorithms. To tackle this challenge, computational intelligence algorithms are applied. In this research, three computational intelligence (CI) algorithms, the evolutionary algorithm (EA) [48, 49], particle swarm optimization (PSO) [17], and harmony search (HS) [35, 36], are used to solve model (4.8). The EA and PSO algorithms have been widely studied in the literature [56, 57]. The HS is a novel algorithm developed in 2001 and has been frequently discussed [35, 58]. The performance of these Three CI algorithms were compared in solving model (4.8).

4.4.1 Algorithm description

The EA algorithm is a meta-heuristic algorithm that simulates the biological evolution process. It produces new genes (solutions) through the recombination and mutation of the existing genes. a_1^{EA} represents size of the initial population, for i = 1, the size of the offspring

population for *i* = 2, mutation parameters for *i* = 3 and 4, and size of tournament selection for *i* = 5. The basic steps of EA are presented next.

Pseudo Code of EA :

1: *Run.* EA($a_1^{EA}, a_2^{EA}, a_3^{EA}, a_4^{EA}, a_5^{EA}$)

2: Initialize a parental population P;

$P = \{\mathbf{x}_i\}, i = 1, 2, ..., a_1^{EA}$;

3: *for* $g = 1 : G$

4: Generate an offspring population P_1;

$P_1 = \{\mathbf{x}_i'\}, i = 1, 2, ..., a_2^{EA}$;

$\mathbf{x}_i' = (\mathbf{x}_j + \mathbf{x}_k)/2; \mathbf{x}_j, \mathbf{x}_k \in P, j \neq k$;

5: *Apply mutation on individuals of* P_1

$\mathbf{x}_i' = \mathbf{x}_i' + N(0, \boldsymbol{\delta}_i)$;

$\boldsymbol{\delta}_i = \boldsymbol{\delta}_i \bullet (e^{N(0,a_3^{EA}) + N_\tau(0,a_4^{EA})} + e^{N(0,a_3^{EA}) + N_\beta(0,a_4^{EA})})^T$;

6: Calculate *fit* of individual of P_1;

7: *Update* P *by tournament selection*;

8: *end*

Figure 4.1. Pseodo Code of EA

The PSO is a population-based meta-heuristic algorithm inspired by the social behavior of flocks of birds and schools of fish. Each particle (bird) is initialized by a vector at position $\mathbf{x}_i$ and a vector with velocity $\mathbf{v}_i$. Each particle wanders in the search space directed by its own velocity, personal searching experience, $\mathbf{x}_{ibest}$, and the searching experience of the swarm, $\mathbf{x}_{gbest}$. a_1^{PSO} is the size of the initial population in PSO. a_i^{PSO} are parameters controlling the velocity of flight in PSO, *i* = 2, 3, 4. The steps of the PSO are shown next.

Pseudo Code of PSO

1: Run.PSO($a_1^{PSO}, a_2^{PSO}, a_3^{PSO}, a_4^{PSO}$)
2: Initialize position and velocity of Particle swarm:
$\mathbf{x}_i, \mathbf{v}_i, i = 1, 2, ..., a_1^{PSO}$;
3: Calculate fit_i, $\mathbf{x}_{ibest}$, fit_{ibest}, $\mathbf{x}_{gbest}$ *and* fit_{gbest}
4: for $g = 1 : G$
5: for $i = 1 : a_1^{PSO}$
6: $\mathbf{v}_i = a_2^{PSO}\mathbf{v}_i + a_3^{PSO} r_1(\mathbf{x}_{ibest} - \mathbf{x}_i) + a_4^{PSO} r_2(\mathbf{x}_{gbest} - \mathbf{x}_i)$;
$r_1 \in U[0,1]; r_2 \in U[0,1]$;
7: $\mathbf{x}_i = \mathbf{x}_i + \mathbf{v}_i$;
8: calculate fit_i;
9: Update fit_{ibest} and $\mathbf{x}_{ibest}$;
10: Update fit_{gbest} and $\mathbf{x}_{gbest}$;
11: end for
12: end for

Figure 4.2. Pseudo Code of PSO

HS mimics the improvisation process in music. The basic steps of HS are shown next. In Step 4 of HS, two methods were used to construct a new harmony: 1) select pitches from harmonies in memory pool; 2) randomly select pitches from the range of the lower boundary, $\mathbf{x}_L$, and the upper boundary, $\mathbf{x}_U$.

a_1^{HS} denotes the size of the initial population in algorithm HS. a_i^{HS} is used to represent the size of the harmony memory for *i* = 2, harmony memory consideration rate (HMCR) for *i* = 3, pitch adjusting rate (PAR) for *i* = 4, and band width for *i* = 5. The pseudo code of HS is represented below.

Pseudo Code of HS :

$1:$ *Run.* $\mathrm{HS}(\mathrm{a}_1^{HS}, \mathrm{a}_2^{HS}, \mathrm{a}_3^{HS}, \mathrm{a}_4^{HS})$

$2:$ Initialize *a memory pool of harmonies*, H;

$\mathrm{H} = \{\mathbf{x}_i\}; i = 1, 2, ..., \mathrm{a}_1^{HS}$

$3:$ *for* $g = 1 : G$

$4:$ *Improvise a new harmony* :

if $rand() < a_2^{HS}$

$i = \mathrm{int}(rand() * \mathrm{a}_1^{HS}) + 1;$

if $rand() < a_3^{HS}$

$\mathbf{y} = \mathbf{x}_i \pm (\mathbf{x}_U - \mathbf{x}_L) * a_4^{HS} * \mathrm{rand}();$

else

$\mathbf{y} = \mathbf{x}_i;$

end

else

$\mathbf{y} = \mathbf{x}_i + (\mathbf{x}_U - \mathbf{x}_L) * \mathrm{rand}();$

end

$5:$ *Substitue the worst harmony in H by the new harmony* $\mathbf{y}$;

$6:$ *end*

Figure 4.3. Pseudo code of HS

4.4.2 Comparative analysis

The performance of the CI algorithms are impacted by their parameter settings. A comprehensive experiment was designed to investigate the performance of the three CI algorithms in solving equation (4.8) based on different combination of parameter settings. The experiment logic is shown in Figure 4.4.

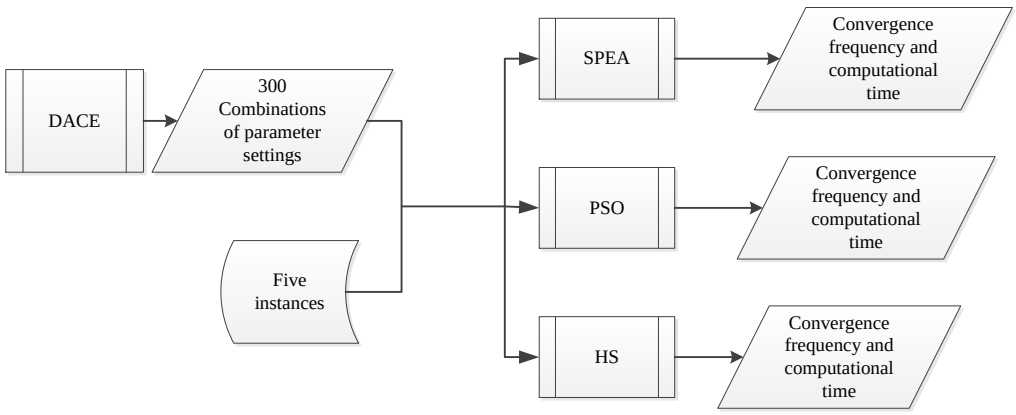

Figure 4.4. Comparative study

Using the Design and Analysis of Computer Experiments (DACE) approach [50], 300 combinations of parameter settings for each algorithm were generated to examine the convergence frequencies and computational time of the three CI algorithms in solving model (4.8). In the experiment, the value of a_1^i for $i = \{EA, PSO, HS\}$ was set to 10. Due to the different properties of the parameters in the three algorithms, two schemes illustrated next were applied to generate parameter settings for the considered CI algorithms:

Design for EA: The EA involves 4 parameters, a_i^{EA}, i = 2, 3, 4, and 5. The a_2^{EA} and a_5^{EA} are integers, $a_2^{EA} = 10, 20, \ldots, 100$ and $a_5^{EA} = 1, 2, \ldots, 10$. The a_3^{EA} and a_4^{EA} are real values, a_3^{EA} and $a_4^{EA} \in [0.1,1]$. Because two continuous parameters are two discrete parameters are involved, a sliced-Latin hypercube design (LHD) [59] was used, which has been proven to provide better statistical properties than a regular LHD [51] when discrete parameters exist. The entire design is a 300-run LHD, which can be decomposed into 100 slices (defined by the combination of a_2^{EA} and a_5^{EA}), and each of them is a small three-run LHD.

Design for PSO and HS: Three parameters have to be determined for both PSO and HS, a_i^{PSO} and a_i^{HS}, i = 2, 3, and 4. Because a_i^{PSO} and a_i^{HS} are continuous parameters, the regular LHD was used for both PSO and HS. Similarly, a 300-run LHD was used.

4.4.3 Summary of computational results

The performances of the three CI algorithms in solving model (4.8) are discussed in this section. Five computational instances were randomly selected from the test dataset. Each algorithm was implemented with 200 iterations for 300 combinations of parameter settings based on five selected computational instances. Two parameters, ε_1 and ε_2 , indicating the performances of the algorithms were recorded. Because the optimization model was proposed for online implementation, an algorithm with a high frequency of convergence and less computational time was desired.

Table 4.4. Summary of experimental results

Algorithms	ε_1	ε_2
EA	250	900
PSO	282	0.26
HS	263	0.04

As shown in Table 4.4, the average computational time of EA is nearly 900 s (15 min), which is not acceptable in online optimization. Both the PSO and HS algorithms show the desired properties: 1) a high convergence frequency, 282/300 and 263/300; 2) and a short computing time, 0.26 and 0.04 s. Therefore, both of them are suitable for online optimization.

4.5 Case studies

The optimization of the HVAC system control using model (4.8) is conducted in this section based on different cases. To validate the effectiveness of the optimized control strategy, a baseline strategy presented in Definition 1 for controlling the same HVAC system at the USB is utilized. The VAV boxes in five rooms are still controlled by the PID controller.

Definition 1. The default controlled setting points of the HVAC system, 2.3 in. WG (0.57 kPa) for SASP-SP and 55 ℉ (12.76 ℃) for DAT-SP, is considered as the baseline strategy.

The optimal control strategy is compared with the baseline strategy to demonstrate the performance improvement in the HVAC system based on three cases. In Case I, minimization of the energy consumption was considered, which means the value of w in (4.8) was set to 1; in Case II, minimization of the energy consumption and minimization of the temperature ramp were considered equally important, and w was set to 0.5; and in Case III, only the minimization of TRR was considered, and w was set to 0.

The HS algorithms was selected to solve model (4.8). The parameter settings of the HS algorithm considered in the cases studies are $a_2^{HS} = 0.88$, $a_3^{HS} = 0.14$, $a_4^{HS} = 0.40$. This combination of parameter settings was selected from the 263 combinations of parameter settings. The maximum number of iterations of the HS algorithm was set to be 200.

The daily data from 8:00 am to 17:45 pm on June 26, 2013, including 39 continuous instances, were used in all of the case studies discussed next.

4.5.1 Case study results

The results of Case I are shown in Figures 4.5, 4.6, and 4.7. Figure 4.5 demonstrates the optimized and baseline energy consumption of the HVAC system. Figure 4.6 compares TRRS, while Figure 4.7 presents the optimized values of the control set points.

As shown in Figure 4.5, significant energy savings are obtained. The baseline strategy is actually optimal for the HVAC system at the beginning because the system needs to be operated at full capacity to decrease the room temperature to a comfortable level after the all night shutdown of the HVAC system at USB. In Figure 4.6, TRR can be slightly larger than 1. This is due to the fact that the room temperature ramp is normalized by dividing it by ξ, which is selected based on historical observations. The phenomenon, a TRR larger than 1, usually occurs at the beginning or end of the working hours for a short time. However, this has negligible

impact on leveraging the two objectives. Overall, the TRR under the proposed control strategy is larger than the TRR under the baseline control strategy, denoting a bigger fluctuation in room temperature. A peak value of TRR is also observed. According to Figure 4.5 and 4.6, it is capable to conclude that minimization of energy consumption only can result in significant energy savings while induce unstable thermal comfort.

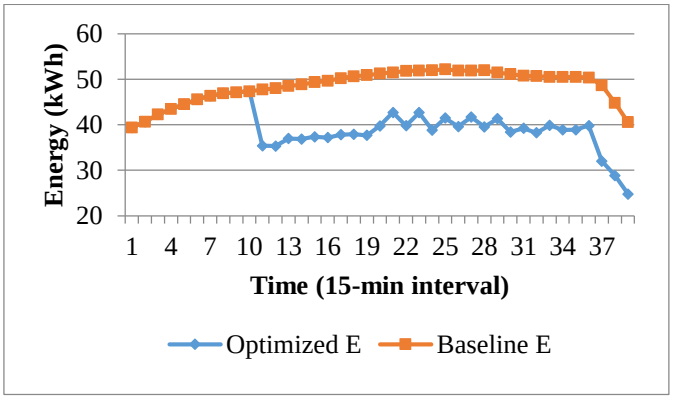

Figure 4.5. Optimized and baseline energy in Case I

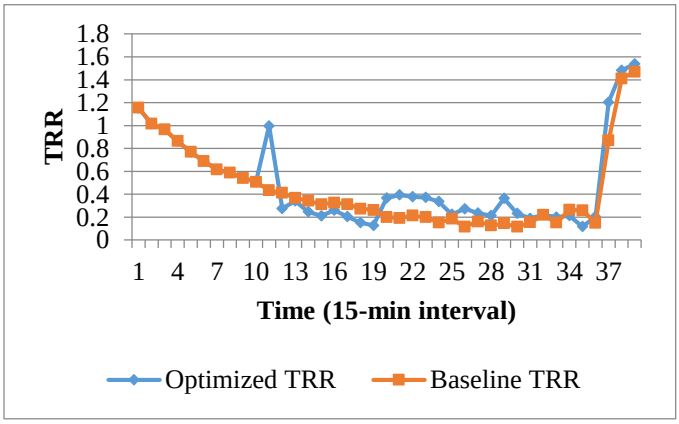

Figure 4.6. Optimized and baseline TRR in Case I

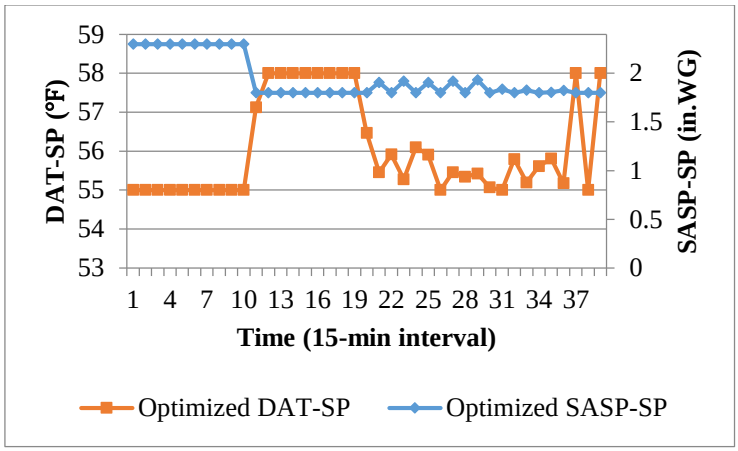

Figure 4.7. Optimized and baseline set points in Case I

In case II, both the energy consumption and room temperature ramp rate were optimized. The energy consumption, TRR, and control set points were computed as shown in Figures 4.8, 4.9, and 4.10, respectively. Compared with the results of Case I, the energy savings are promising, while the fluctuation of the control parameters is reduced. By controlling the TRR, the value of optimized TRR becomes smaller compared to the baseline TRR.

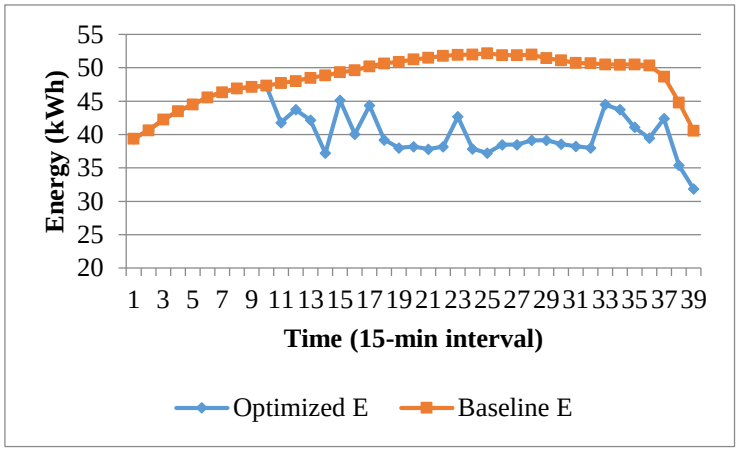

Figure 4.8. Optimized and baseline energy in Case II

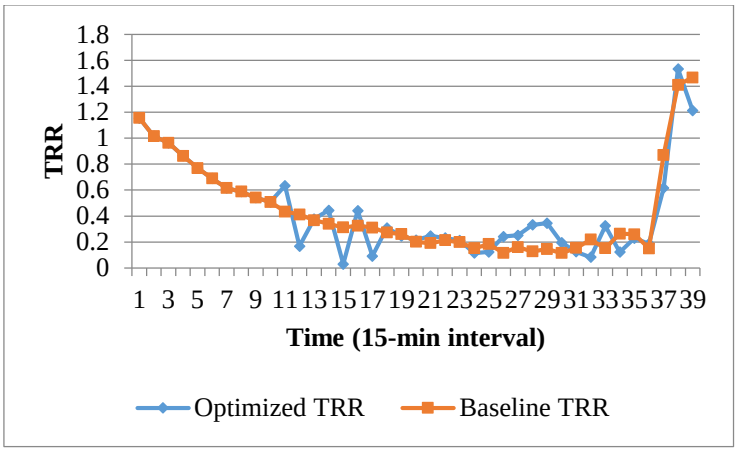

Figure 4.9. Optimized and baseline TRR in Case II

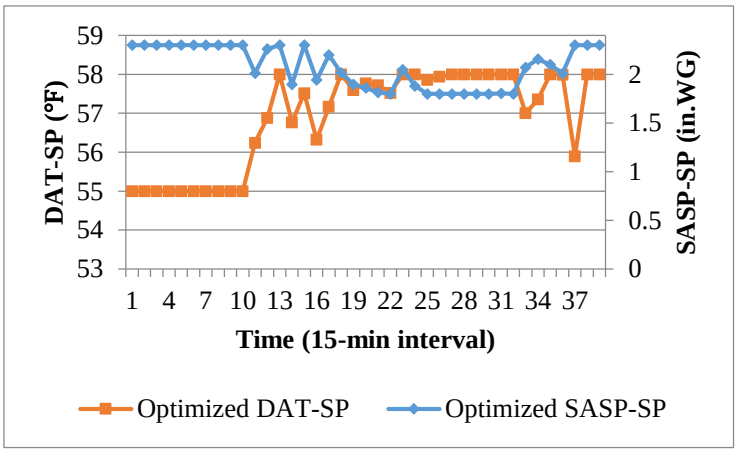

Figure 4.10. Optimized and baseline set points in Case II

In Case III, only the room temperature ramp was minimized. As shown in Figures 4.11 and 4.12, considerable energy savings are observed, which indicated that it is a waste of energy to constantly run the HVAC system at full capacity. The optimized TRR is kept at a lower value most of the time, compared with the TRR under the baseline strategy.

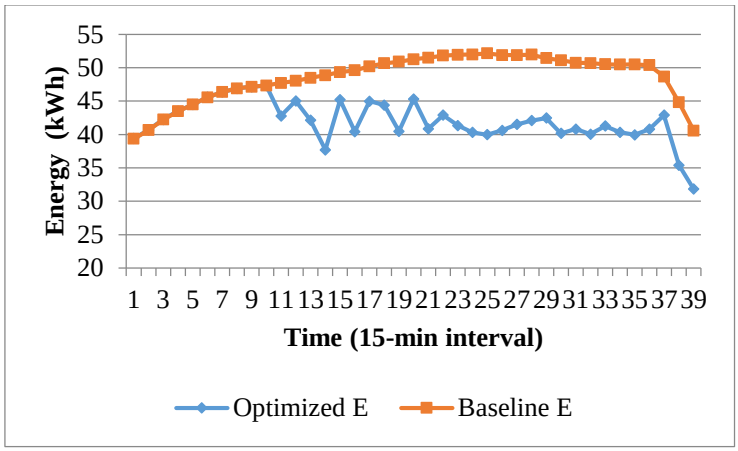

Figure 4.11. Optimized and baseline energy in Case III

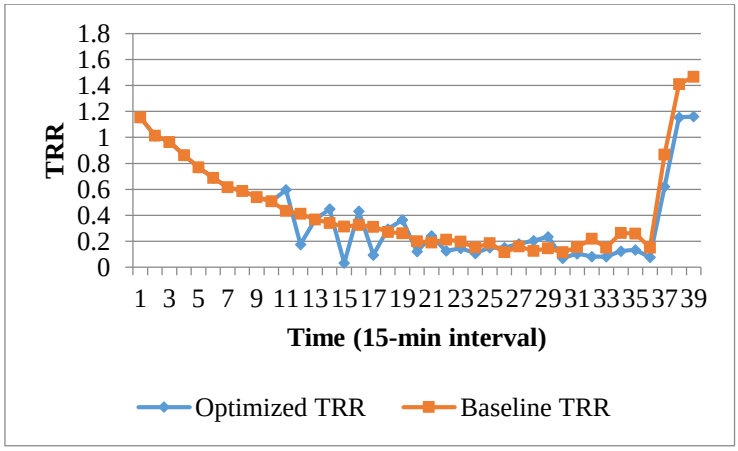

Figure 4.12. Optimized and baseline TRR in Case III

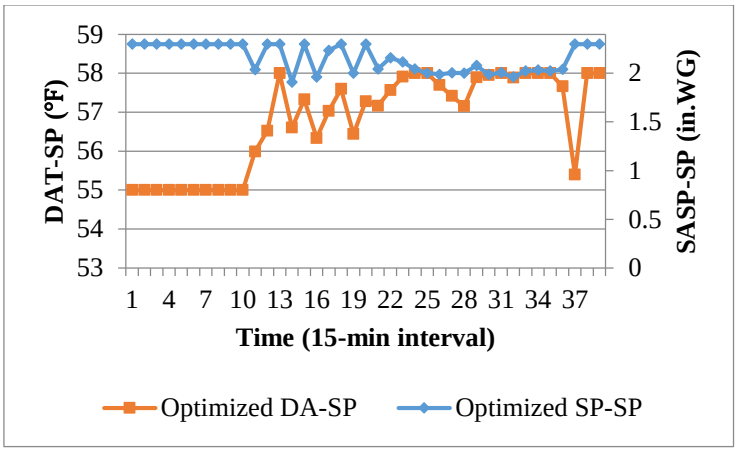

Figure 4.13. Optimized and baseline set points in Case III

4.5.2 Summary of case studies

The results of Case I, II, and III are summarized in Table 4.5. The optimized energy consumption and room temperature ramp rate are compared with the baseline values. The gains in energy consumption and room temperature ramp rate are defined in equation (4.4).

$$Gain = \frac{Baseline\ value - Optimized\ value}{Baseline\ value} \tag{4.9}$$

In Case I in Table 4.5, the energy consumption is reduced by 18.50%, while the temperature ramp rate increases to 10.20%. In Case II, the energy consumption and room temperature were equally weighted. Thus, a 15.70% energy savings is achieved with a temperature ramp rate similar to the baseline model. Minimization of the room temperature ramp rate led to a 9.80% decrease in the ramp rate, indicating better stability of the thermal comfort. The results in Table 4.5 indicate that focusing on minimizing the room temperature ramp rate leads to smaller gains in energy savings.

The optimized energy consumptions for Case I and Case II are compared in Figure 4.14. During some time intervals, models that considered both the energy consumption and room

temperature ramp rate led to smaller energy savings than the model minimizing the energy consumption. For the HVAC system discussed in this paper, the results in Table 4.5 show that optimizing the energy consumption only leads to the largest energy savings.

Table 4.5. Summary of case study results

Power	Case 1	Case 2	Case 3
Optimized	1542.2	1595.3	1637.3
Baseline	1893.4	1893.4	1893.4
Gain	18.50%	15.70%	13.50%
Temperature Ramp	Case 1	Case 2	Case 3
Optimized	19.3	17.4	15.8
Baseline	17.5	17.5	17.5
Gain	-10.20%	0.60%	9.80%

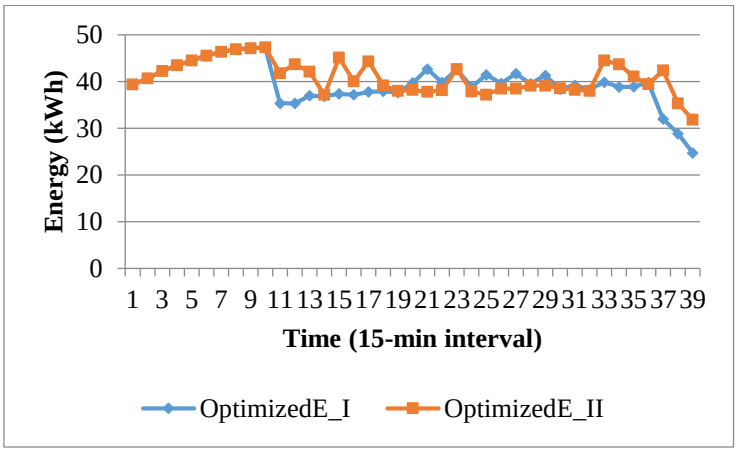

Figure 4.14. Optimized energy in Case I and Case II

4.6 Conclusion

In this chapter, an optimization model for minimizing the energy consumption and preserving the thermal comfort of an office space was proposed. Data-driven methods were derived from data collected from an experiment.

Three computational intelligence algorithms were introduced to solve the proposed optimization model. The performances of these algorithms were impacted by the parameter settings. To evaluate and compare the general performances of the three algorithms, a Design and Analysis of Computer Experiment technique was utilized to generate 300 parameter settings for each computational intelligence algorithm. The performance of each algorithm was evaluated by computing five instances from the dataset based on 300 parameter settings. Both of the harmony search algorithm and particle swarm optimization were found to be suitable for real-time optimization because of their computational speed and quality of solutions.

Optimization of the HVAC system performance was analyzed based on the proposed optimization model for three cases. The computational results indicated that energy savings could be achieved by optimizing the settings for the supply air static pressure set point and discharged air temperature set point. Additionally, the introduction of room temperature ramp control to the objective function was beneficial for smoothing the control settings of the set points and achieving better room thermal comfort.

CHAPTER 5

CONCLUSION

In this Thesis, data mining method has been applied to optimize the operation of a pump system in wastewater treatment plant, and management of a HVAC system in commercial buildings by deriving system models from historical models. Optimization model integrating system models and constraints were constructed and solved to achieve goal of reducing energy consumption. In Chapter 1, current research on optimizing the two systems, pump systems and HVAC systems, are reviewed. It also reviewed application of data mining method in industrial fields.

In Chapter 2, pump system in a wastewater treatment plant was investigated. Energy consumption models and outflow rate models for different pump system configurations were built using historical data collected. Optimization model minimizing energy consumption and considering control of level of wet well chamber was built. An improved harmony search algorithm was used to solve optimization model. Around 16% percentage of energy consumption savings were achieved in Low, Medium, and High inflow rate scenarios simulation.

In Chapter 3, a pilot study was carried out, optimizing operations of pump system considering maintenance in a wastewater treatment plant. Multi-input multi-output multiple layers perceptron neural networks were used to build energy consumption models and outflow rate models simultaneously, which showed slight better model accuracy than build models separately. The maintenance decision process of pump was formulated as a Markov decision process. Optimization model minimizing overall cost, including operation cost and maintenance cost, was constructed. Due to the complexity of optimization model, extended particle swarm optimization algorithm was proposed to solve it, and optimization strategies were provided for considered Low, Medium, and High inflow rate scenarios.

In Chapter 4, Optimization of management of HVAC system in a commercial building was studied. Both energy consumption and quality of control buildings were considered to

minimize energy consumption and maintain comfort of people in buildings. Temperature ramp rate (TRR) was introduced to control the vibration of room temperature, which also proved the potential of saving more energy in long time horizon by considering both energy consumption and TRR than only consider energy consumption. Above 10% energy consumption savings can be achieved in simulation study.

Applicability for implementation should be studied in future research. Although data-mining method can generalize knowledge learned from data, it is potential to suffer system damage if situations out of training data happen. Therefore, validation and risk analysis of these models should be further carried out for application. On the other hand, the system may change gradually, it would be more worthwhile if system models developed by data mining method can be updated online.

APPENDIX A

METRICS FOR EVALUATION OF PREDICTIVE MODELS

The prediction accuracy of the developed predictive models in Chapters 2 to 4 were measured using the following four metrics: 1) the mean absolute error (MAE), 2) the standard deviation of the absolute error (sdAE), 3) the mean absolute percentage error (MAPE), and 4) the standard deviation of the absolute percentage error (sdAPE). These metrics are expressed in (A.1) – (A.4).

$$\text{MAE} = (1/n)\sum_{k=1}^{n}\left|\hat{y}_k - y_k\right| \tag{A.1}$$

$$\text{sdAE} = \sqrt{(1/n)\sum_{k=1}^{n}(\left|\hat{y}_k - y_k\right| - (1/n)\sum_{k=1}^{n}\left|\hat{y}_k - y_k\right|)^2} \tag{A.2}$$

$$\text{MAPE} = (1/n)\sum_{k=1}^{n}\left|(\hat{y}_k - y_k)/y_k\right| \tag{A.3}$$

$$\text{sdAPE} = \sqrt{(1/n)\sum_{k=1}^{n}(\left|(\hat{y}_k - y_k)/y_k\right| - (1/n)\sum_{k=1}^{n}\left|(\hat{y}_k - y_k)/y_k\right|)^2} \tag{A.4}$$

where y is the measured value, $\hat{y}$ is the predicted value, k is the index of the data points, and n is the total number of data points.

REFERENCES

[1] D. J. Sailor, "A green roof model for building energy simulation programs," *Energy and Buildings*, Vol. 40, No. 8, pp. 1466-1478, 2008.

[2] G. C. Bakos, M. Soursos, and N. F. Tsagas, "Technoeconomic assessment of a building-integrated PV system for electrical energy saving in residential sector," *Energy and Buildings*, Vol. 35, No. 8, pp. 757-762, 2003.

[3] L. Perez-Lombard, J. Ortiz, and I. R. Maestre, "The map of vienergy flow in HVAC systems," *Applied Energy*, Vol. 88, No. 12, pp. 5020-5031, 2011.

[4] Electric Power Research Institued, "Energy Audit Manual of Water/Wastewater Facilities", Electric Power Research Institute, Palo Alto, CA, 1999.

[5] D. Denig-Chakroff, National Regulatory Research Institute, "Reducting Electricity Used for Water Production: Questions State Commissions Should Ask Regulated Utilities," June 13, 2008, p.5; see *http://nrri.org/pubs/water/reducing_electricity_used_for_water_08-06.pdf*

[6] L. Perez-Lombard, J. Ortiz, C. Pout, A review on building energy consumption information, Energy and Buidings 40 (3) (2008) 394-8.

[7] E. Alperovits and U. Shamir, "Design of Optimal Water Distribution System," *Water Resources Research*, Vol. 13, No. 6, pp. 885-900, 1977.

[8] M. Cunha and J. Sousa, "Water Distribution Network Design Optimization: Simulated Annealing Approach," *ASCE Journal of Water Resources Planning and Management*, Vol. 125, No. 4, pp. 215-221, 1999.

[9] K. Lansey and L. Mayes, "Optimization Model for Water Distribution System Design, " *ASCE Journal of Hydraulic Engineering*, Vol. 115, No. 10, pp. 1401-1418, 1989.

[10] Z. Ma and S. Wang, "Energy efficient control of variable speed pumps in complex building central air-conditioning systems," *Energy and Buildings*, Vol. 41, No. 2, pp. 197-206, 2009.

[11] X. Zhuan and X. Xia, "Development of Efficient Model Predictive Control Strategy for Cost-Optimal Operation of a Water Pumping System," *IEEE Transactions on Control Systems Technology*, Vol. 21, No. 4, pp. 1449-1454, 2013.

[12] L. Ormsbee and K. Lansey, "Optimal control of water supply pumping systems," *ASCE Journal of Water Resources Planning and Management*, Vol. 120, No .2, pp. 237-252, 1994.

[13] Y. Wang, T. Chang, and J. Chen, "An enhanced genetic algorithm for bi-objective pump scheduling in water supply," *Expert Systems with Applications*, Vol. 36, No. 7, pp. 10249-10258, 2009.

[14] X. Zhuan and X. Xia, "Optimal operation scheduling of a pumping station with multiple pumps," *Applied Energy*, Vol. 104, pp. 250-257, 2013.

[15] Z. Zhang, Y. Zeng, and A. Kusiak, "Minimizing Pump Energy in a Wastewater Processing Plant," *Energy*, Vol. 47, No. 1, pp. 505-514, 2012.

[16] A. S. Fraser, "Simulation of genetic systems by automatic digital computers. I. Introduction," *Australian Journal of Biological Science*, Vol. 10, pp. 484-491, 1957.

[17] J. Kennedy and R. C. Eberhart, "Particle swarm optimization," *IEEE International Conference on Neural Networks*, pp. 1942-1948, 1995

[18] M. Dorigo andL. M. Gambardella, "Ant Colony System: A Cooperative Learning Approach to the Traveling Salesman Problem," *IEEE Transactions on Evolutionary Computation*, Vol. 1, No. 1, pp. 53-66, 1997.

[19] J. E. van Zyl, D. A. Savic, and G. A. Walters, "Operational optimization of water distribution systems using a hybrid genetic algorithm," *ASCE Journal of Water Resources Planning and Management*, Vol. 130, No. 2, pp. 160-170, 2004.

[20] M. Hajji, A. Fares, F. Glover, and O. Driss, "Water Pump Scheduling System Using Scatter Search, Tabu Search and Neural Networks the Case of Bouregreg Water System in Morocco," *ASCE World Environmental and Water Resources Congress*, pp. 822-832, 2010.

[21] M. Lopez-lbanez, T. D. Prasad, and B. Paechter, "Ant colony optimization for optimal control of pumps in water distribution networks," *ASCE Journal of Water Resources Planning and Management*, Vol. 134, No. 4, pp. 337-346, 2008.

[22] S.W. Wang, Z.J. Ma, Supervisory and optimal control of building HVAC systems: a review, *HVAC&R* Research, Vol. 14, No. 1, 2007

[23] R. Alcalá, J. Casillas, O. Cordo´, A. Gonza´ lez, and F. Herrera, "A genetic rule weighting and selection process for fuzzy control of heating, ventilating and air conditioning systems", *Engineering Applications of Artificial Intelligence*, Vol.18, No. 3, pp. 279-296, 2005.

[24] L. Lu, W. Cai, Y.S. Chai, and L. Xie, "Global optimization for overall HVAC systems - Part I problem formulation and analysis," *Energy Conversion and Management*, Vol. 46, No. 7–8, pp. 999–1014, 2005.

[25] L. Lu, W. Cai, Y.S. Chai, and L. Xie, "Global optimization for overall HVAC systems - part II problem solution and simulations," *Energy Conversion and Management*, Vol. 46, No. 7–8, pp. 1015–1028, 2005.

[26] S. Wang and X. Jin, "Model-based optimal control of VAV air-conditioning system using genetic algorithm," *Building and Environment*, Vol. 35, No. 6, pp. 471-487, 2000.

[27] N. Nassif, S. Moujaes, "A cost-effective operating strategy to reduce energy consumption in a HVAC system," *International Journal of Energy Research*, Vol. 32, No. 6, pp.543-558, 2008.

[28] A. Kusiak, and G. Xu, "Modeling and optimization of HVAC systems using a dynamic neural network," *Energy*, Vol. 42, pp. 241-250, 2012.

[29] U. Fayyad, G. Piatetsky-Shapiro, and P. Smyth, "The KDD process for extracting useful knowledge from volumes of data," *Communications of the ACM*, Vol. 39, No. 11, 1996.

[30] G. Koksal, I. Batmaz, and M.C Testik, "A review of data mining application for quality improvement in manufacturing industry," *Expert Systems with Applications*, Vol. 38, pp. 13448 – 13467, 2011.

[31] F.Xiao, and C. Fan, "Data mining in building automation systems for improving building operational performance," *Energy and Buildings*, Vol. 75, pp. 109-118, 2014.

[32] I. Colak, S. Sagiroglu, and M. Yesilbudak, "Data mining and wind power prediction: a literature review," *Renewable Energy*, Vol.46, pp. 241-247, 2012.

[33] A. Kusiak, and W. Li, "The prediction and diagnosis of wind turbine faults," *Renewable Energy*, Vol. 36, pp. 16 – 23, 2012

[34] J.S. Chou, Y.C. Hsu, and L.T. Lin, "Smart meter monitoring and data mining techniques for predicting refrigeration system performance," *Expert Systems with Applications*, Vol. 41, pp.2144 – 2156, 2014.

[35] M. Madhdavi, M. Fesanghary, and E. Damangir, "An improved harmony search algorithm for solving optimization problems", *Applied Mathematics and Computation*, Vol. 188, No. 2, pp. 1567-1579, 2007.

[36] Z.W. Geem, J.H. Kim, and G.V. Loganathan, "A new heuristic optimization algorithm: harmony search," *Simulation*, Vol. 76, No. 2, pp. 60–68, 2001.

[37] A. Kusiak, Z. Zhang, and G. Xu, "Minimization of Wind Farm Operational Cost Based on Data-Driven Models," *IEEE Transactions on Sustainable Energy*, Vol. 4, No. 3, pp. 756-764, 2013.

[38] A. Verma, Z. Zhang, and A. Kusiak, "Modeling and Prediction of Gearbox Faults With Data-Mining Algorithms," *ASME Journal of Solar Energy Engineering*, Vol. 135, No. 3, pp. 031007-1-031007-11, 2013.

[39] R. Bellman, "A Markov decision process," *Journal of Mathematics and Mechanics*, Vol. 6, pp. 679-693, 1957.

[40] S. K. Abeygunawardane, P. Jirutitijaroen, and H. Xu, "Adaptive Maintenance Policies for Aging Devices Using a Markov Decision Process," *IEEE Transactions on Power Systems*, Vol. 28, No. 3, pp. 3194-3203, 2013.

[41] Y. Wu and H. Zhao, "Optimization maintenance of wind turbines using Markov decision processes," *IEEE 2010 International Conference on Power System Technology*, pp. 1-6, 2010.

[42] B. Baron, C. Von Lucken, and A. Sotelo, "Multi-objective pump scheduling optimization using evolutionary strategies," *Advance in Engineering Software*, Vol. 36, No. 1, pp. 39 – 47, 2005.

[43] Z. Yang and H. Borsting, "Optimal scheduling and control of a multi-pump boosting system," *IEEE 2010 International Conference on Control Applications*, pp. 2071-2076, 2010.

[44] Z. Zhang and A. Kusiak, "Models for Optimization of Energy Consumption of Pumps in a Wastewater Processing Plant," *ASCE Journal of Energy Engineering*, Vol. 137, No. 4, pp. 159-168, 2011.

[45] H. Siegelmann and E. Sontag, "Analog computation via neural networks," *Theoretical Computer Science*, Vol. 131, No. 2, pp. 331-60, 1994.

[46] D. H. Martin, "The essence of invexity," *Journal of Optimization Theory and Applications*, Vol. 47, No. 1, pp. 65-76, 1985.

[47] J. Kennedy and R. C. Eberhart, "A discrete binary version of the particle swarm algorithm," *IEEE Conference on Systems, Mans, and Cybernetics*, pp. 4104-4109, 1997.

[48] E. Zitzler and L. Thiele, "Multiobjective Evolutionary Algorithms: A Comparative Case Study and the Strength Pareto Evolutionary Algorithm," *IEEE Transactions on Evolutionary Computation*, Vol. 3, No. 4, pp. 257-271, 1999.

[49] K. Deb, A. Pratap, S. Agarwal, and T. Meyarivan, "A fast and elitist multiobjective genetic algorithm: NSGA-II," *IEEE Transactions on Evolutionary Computation*, Vol. 6, No. 2, pp. 182-197, 2002.

[50] T. J. Santner, B. J. Williams, W. I. Notz, The Design and Analysis of Computer Experiments, New York, 2003.

[51] M. D. Mckay, R. J. Beckman, and W. I. Conover, "A comparison of three methods for selecting values of input variables in the analysis of output from a computer code," *Technometrics*, Vol. 42, No. 1, pp. 55-61, 2000.

[52] F. Fine, Feedforward Neural Network Methodology, New York, 1999.

[53] S. Haykin, Neural Networks: A Comprehensive Foundation, Prentice Hall, 1998.

[54] A. Kusiak, G. Xu, and F. Tang, "Optimization of an HVAC System with a Strength Multi-objective Particle Swarm Algorithm," *Energy*, Vol. 35, No. 10, pp. 5935-5943, 2011.

[55] A. Kusiak, Y. Zeng, and G. Xu, "Minimizing Energy Consumption of an Air Handling Unit with a Computational Intelligence Approach," *Energy and Buildings*, Vol. 60, No. 1, pp. 355-363, 2013.

[56] M. A. Abido, "Optimal design of power-system stabilizers using particle swarm optimization," *IEEE Transactions on Energy Conversion*, Vol. 17, No. 3, pp. 406-413, 2002.

[57] A. Kusiak, Z. Zhang, and M. Y. Li, "Optimization of Wind Turbine Performance with Data-Driven Models," *IEEE Transactions on Sustainable Energy*, Vol. 1, No. 2, pp. 66-76, 2010.

[58] L. S. Coelho and V. C. Mariani, "An improved harmony search algorithm for power economic load dispatch," *Energy Conversion and Management*, Vol. 50, No. 10, pp. 2522-2526, 2009.

[59] P. Qian, "Sliced Latin Hypercube Designs," *Journal of the American Statistical Association*, Vol. 107, No. 497, pp. 393-399, 2012.